

UNIVERSIDADE FEDERAL DE MINAS GERAIS  
FACULDADE DE MEDICINA  
PROGRAMA DE PÓS-GRADUAÇÃO EM MEDICINA MOLECULAR

Eduardo de Souza Nicolau

**AN EXPERIMENTAL MODEL OF TRANSCRANIAL DIRECT CURRENT  
STIMULATION (tDCS) IN MICE**

**UM MODELO EXPERIMENTAL DE ESTIMULAÇÃO TRANSCRANIANA POR CORRENTE CONTÍNUA EM  
CAMUNDONGOS**

Belo Horizonte  
2018

Eduardo de Souza Nicolau

**AN EXPERIMENTAL MODEL OF TRANSCRANIAL DIRECT CURRENT  
STIMULATION (tDCS) IN MICE**

**UM MODELO EXPERIMENTAL DE ESTIMULAÇÃO TRANSCRANIANA POR CORRENTE CONTÍNUA EM  
CAMUNDONGOS**

Dissertação apresentada ao Programa de Pós-graduação em Medicina Molecular da Faculdade de Medicina da UFMG como requisito parcial para obtenção de título de mestre.

Orientador: Professor Marco Aurélio Romano Silva  
(MD-PhD)

Coorientador: Dr. Luiz Alexandre Viana Magno  
(PhD)

Belo Horizonte

2018

Ficha de identificação da obra elaborada pelo autor, através do  
Programa de Geração Automática da Biblioteca Universitária da UFMG

Nicolau, Eduardo de Souza

UM MODELO EXPERIMENTAL DE ESTIMULAÇÃO  
TRANSCRANIANA POR CORRENTE CONTÍNUA EM  
CAMUNDONGOS [manuscrito] / Eduardo de Souza Nicolau. -  
2018.

72 f. : il.

Orientador: Marco Aurélio Romano-Silva.

Coorientador: Luiz Alexandre Viana Magno.

Dissertação (Mestrado) - Universidade Federal de Minas  
Gerais, Faculdade de Medicina.

1.Estimulação Transcraniana. 2.Modelo Animal. 3.Mecanismos  
de Ação. 4.Efeitos Evocados. I.Romano-Silva, Marco Aurélio.  
II.Magno, Luiz Alexandre Viana. III.Universidade Federal de  
Minas Gerais. Faculdade de Medicina. IV.Título.



UNIVERSIDADE FEDERAL DE MINAS GERAIS

PROGRAMA DE PÓS-GRADUAÇÃO EM MEDICINA MOLECULAR



## FOLHA DE APROVAÇÃO

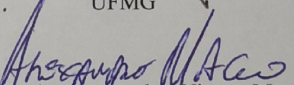
**UM MODELO EXPERIMENTAL DE ESTIMULAÇÃO TRANSCRANIANA POR  
CORRENTE CONTÍNUA EM CAMUNDONGOS**

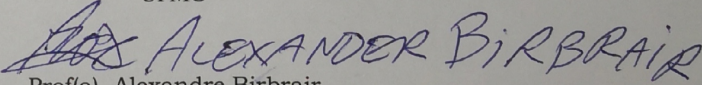
**EDUARDO DE SOUZA NICOLAU**

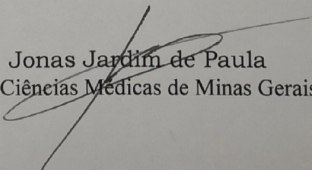
Dissertação submetida à Banca Examinadora designada pelo Colegiado do Programa de Pós-Graduação em MEDICINA MOLECULAR, como requisito para obtenção do grau de Mestre em MEDICINA MOLECULAR, área de concentração MEDICINA MOLECULAR.

Aprovada em 01 de novembro de 2018, pela banca constituída pelos

  
Prof(a). Marco Aurélio Romano Silva - Orientador  
UFMG

  
Prof(a). Luiz Alexandre Viana Magno  
UFMG

  
Prof(a). Alexandre Birbrair  
UFMG

  
Prof(a). Jonas Jardim de Paula  
Faculdade de Ciências Médicas de Minas Gerais

Belo Horizonte, 1 de novembro de 2018.

## ABSTRACT

Transcranial direct current stimulation (tDCS) is a non-pharmacological and non-invasive therapeutic technique which principals consist in delivering low intensity currents to the human scalp evoking neuronal excitation (anodal stimulation) or inhibition (cathodal stimulation). Furthermore, it has been proposed as an alternative or complementary treatment for psychiatric diseases. It has also been used as a human enhancement therapy, improving motor and cognitive tasks. Despite an increase in clinical studies, there is still much to be learned from its overall mechanisms. Unfortunately, there are limitations that hinders further investigation of tDCS effects in the human brain. Therefore, the use of animal-tDCS models are of utmost importance and may bring great insight. In this work we proposed an easy and fast to execute tDCS model, supported by efficiency markers (genetic expression alterations) and data related to further investigating tDCS mechanisms (molecular and behavioral profiles). Data showed a viable stimulation model, executable in up to 30 minutes and resistant to longer periods of stimulation (5-day contact quality,  $p=n.s.$ , 10-day contact quality  $p=n.s.$ ). Concurrently, anodal tDCS over cortex M1 and M2 of 5 days (1-session/day, 10 min. 350  $\mu A$ ) increased the expression of *BDNF* ( $p=0.0081$ ), a strongly cognitive associated gene and *GFAP* ( $p=0.0108$ ) an astrocyte marker, expression levels in stimulated (tDCS) vs. non-stimulated (Sham) mice. This data was found to be specific for this protocol, whereas increase stimulation sessions and session disruption did not evoke any molecular alterations. In addition, gene expression alterations were restricted to these genes, once none of the other 8 neuronal associated genes tested suffered modulation. This model also presented enhanced learning performance in the Barnes Maze task, with a decrease in errors ( $p=0.0463$ ), time taken ( $p=0.0409$ ) and distance traveled ( $p=0.0105$ ) to execute the task. Interestingly, the increased performance was attributed to an adaptation in more efficient (direct and serial –  $p=0.0003$ ) strategies by the stimulated animals. Glutamate concentrations were also assessed but did not present significant differences. Overall, the presented model should attend as a future reference in animal model development and serve to investigate and describe additional tDCS underlying mechanisms, bringing light to tDCS real potential.

Key-Words: Transcranial Direct Current Stimulation (tDCS), animal model validation, gene expression, behavioral alterations

## RESUMO

A estimulação transcraniana por corrente contínua (ETCC) é uma técnica terapêutica, não-farmacológica e não invasiva, que parte do princípio da aplicação de correntes elétricas de baixa intensidade aplicadas diretamente a cabeça humana com o intuito de evocar atividades neuronais excitatórias (estimulação anódica) e inibitórias (estimulação catódica). No mais, a ETCC vem sendo proposta como tratamento alternativo ou complementar para tratar diversas doenças neuropsiquiátricas e podendo também ser direcionada para o melhoramento humano em funções motoras e cognitivas. No entanto, apesar do aumento no número de estudos em ETCC, seus mecanismos ainda são vastamente desconhecidos. Infelizmente, existem limitações que impedem investigações mais profundas dos efeitos de tDCS no cérebro humano. Sendo assim, o uso de modelos animais é de extrema importância. Neste trabalho, propomos um modelo animal cirúrgico de tDCS, de rápida e fácil execução, suportado por marcadores gênicos de eficiência e dados adicionais para a investigação dos mecanismos da ETCC. As análises de dados mostraram que o modelo proposto é viável, com execução de até 30 minutos, e resistente à longos períodos de estimulação (contato de qualidade do grupo de 5 dias –  $p=n.s.$ , e do grupo de 10 dias –  $p=n.s.$ ). No mais, estimulação anódica sobre as regiões M1 e M2 por 5 dias (1 sessão/di, 10 min. 350  $\mu A$ ), induziu o aumento significativo de *BDNF* ( $p=0.0081$ ), um gene fortemente associado com desempenho cognitivo e de *GFAP* ( $p=0.0108$ ) um marcador de astrócitos, nos animais estimulados (tDCS) em relação aos animais não-estimulados (Sham). Esses dados foram considerados específicos para este protocolo, pois, um aumento das sessões de estimulação e a interrupção de sessão não evocaram quaisquer alterações moleculares. Além disso, alterações de expressão gênica foram restritas a esses genes, uma vez que nenhum dos outros 8 genes neuronais foram modulados. Este modelo, também apresentou melhor desempenho de aprendizagem na tarefa Barnes Maze, com diminuição de erros ( $p=0.0463$ ), tempo gasto ( $p=0.0409$ ) e distância percorrida ( $p=0.0105$ ) para executar a tarefa. Curiosamente, o aumento do desempenho foi atribuído a uma adaptação mais eficiente (direta e seriada  $p=0.0003$ ) na estratégias adotada pelos animais estimulados. As concentrações de glutamato também foram avaliadas, mas não apresentaram diferenças significativas. Em geral, o modelo

apresentado tem potencial de referência futura no desenvolvimento de modelos animais e podendo servir ainda para investigar e descrever mecanismos subjacentes adicionais de ETCC, trazendo luz ao seu real potencial da.

Palavras-chave: Estimulação de Corrente Direta Transcraniana (ETCC), validação de modelo animal, expressão gênica, alterações comportamentais

## LIST OF FIGURES

Fig. 1. Human and Mouse tDCS layout.....	15
Fig. 2. tDCS underlying mechanism.....	18
Fig. 3. Experimental timeline of group 5/1.....	30
Fig. 4. Experimental timeline of group 5/5.....	31
Fig. 5. Experimental timeline of group 10/1.....	32
Fig. 6. Experimental timeline of group task-paired.....	33
Fig. 7. Illustration of the Barnes Maze Apparatus.....	37
Fig. 8. Illustration of glutamate kinetics for total quantification.....	39
Fig. 9. Gene expression changes evoked by tDCS in group 5/1.....	43
Fig. 10. Gene expression changes evoked by tDCS in group 5/5.....	44
Fig. 11. Gene expression changes evoked by tDCS in group 10/1.....	45
Fig. 12. Task-paired habituation performance.....	46
Fig. 13. Task-paired primary and total errors.....	47-48
Fig. 14. Task-paired primary and total latency.....	49
Fig. 15. Task-paired primary and total distance traveled.....	51
Fig. 16. Task-paired mean speed performance.....	52
Fig. 17. Task-paired general use of strategies.....	53
Fig. 18. Strategy efficiency stratification by primary errors, latency and distance traveled.....	54
Fig. 19. Strategy use of tDCS vs. Sham.....	55
Fig. 20. Gene expression changes evoked by tDCS in group task-paired.....	56
Fig. 21. Total cortical glutamate determination.....	57
Fig. 22. Contact quality for groups 5/1, 5/5, 10/1 and task-paired.....	58-60



**LIST OF TABLES**

Table 1. Genes and primers used for qPCR.....34

## LIST OF ACRONYMS AND INITIALS

$\mu\text{A}$	Micro Ampers
A.D.	Anno Domini
AD	Alzheimer's Disease
AMPA	$\alpha$ -amino-3-hydroxy-5-methyl-4-isoxazolepropionic acid receptor
ARC	activity-regulated cytoskeleton
AT	Anneling Temperature
B.C.	Before Christ
BDNF	Brain-derived neurotrophic factor
$\text{Ca}^{++}$	Calcium
$\text{CaCl}_2 \cdot 2\text{H}_2\text{O}$	Double Hydrated Calcium chloride
CAMKII $\alpha$	Calcium/calmodulin-dependent protein kinase II
Cav	Caveolin
CDK5	cyclin dependent kinase 5
cDNA	Complementary Deoxyribonucleic acid
cFos	Fos proto-oncogene
COMT	Catechol-O-methyltransferase
Cq	Cycle Quantitation
GABA	$\gamma$ -aminobutyric acid
GAD67	glutamate decarboxylase 1
GDH	Glutamate Dehydrogenase
GFAP	glial fibrillary acidic protein
Gria1	glutamate receptor, ionotropic, AMPA1 (alpha 1)
HDRS	Hamilton Depression Rating Scale
KCl	Potassium chloride
KRH	Krebs-Ringer-Hepes
LTD	Long-term depression
LTP	Long-term potentiation
M1	Motor Cortex 1
M2	Motor Cortex 2
$\text{Mg}^{++}$	Magnesium
$\text{MgCl}_2 \cdot 6\text{H}_2\text{O}$	Hexahydrated Magnesium chloride
mRNA	Messenger Ribonucleic Acid
MS	Multiple Sclerosis
N.S.	Not Significant
$\text{Na}^+$	Sodium
NaCl	Sodium chloride
NADP	$\beta$ -Nicotinamide adenine dinucleotide phosphate
NC	Number of Cycles
NCBI	National Center for Biotechnology Information
NMDAR	N-methyl-D-aspartate receptor

PD	Parkinson's Disease
PSD	Post-synaptic density
PSD95	discs large MAGUK scaffold protein 4
qPCR	Quantitative Real Time Polymerase Chain Reaction
RFU	Relative Florscent Units
RNA	Ribonucleic acid
RPL13A	ribosomal protein
RPM	Rotations Per Minute
S.D.	Standard Deviation
S.E.M	Standard Error Mean
SYN1	synapsin I
tDCS	Transcranial direct current stimulation
tES	Transcranial electrical stimulation
Trk	Tropomyosin-receptor kinase
VRM	Visual Recognition Memory task
WRT	Word Recognition Task

## SUMMARY

1.0 INTRODUCTION .....	11
2.0 OBJECTIVES .....	19
2.1 Overall Objectives.....	20
2.2.0 Specific Objectives.....	20
3.0 PUBLISHED ARTICLE .....	21
4.0 MATERIALS AND METHODS.....	29
4.1.0 tDCS procedures and groups. ....	30
4.2.0 Cervical Dislocation. ....	34
4.3.0 Tissue extraction and separation. ....	34
4.4.0 Ribonucleic acid (RNA) Extraction and Complementary Deoxyribonucleic acid (cDNA) synthesis. ....	35
4.5.0 Quantitative Real Time Polymerase Chain Reaction (qPCR).....	35
4.6.0 Barnes Maze (Behavioral Assessment).....	36
4.7.0 Total Glutamate determination.....	38
5.0 RESULTS .....	41
5.1.0 tDCS gene expression profile. ....	42
5.2.0 tDCS task-paired group behavioral and genetic profile. ....	46
5.2.0 Cortical assessment of total glutamate determination. ....	56
5.3.0 tDCS implant and electrode viability. ....	58
6.0 DISCUSSION .....	61
6.1.0 tDCS induces gene expression alterations. ....	62
6.2.0 tDCS induces learning enhancement. ....	63
6.3.0 tDCS does not affect total glutamate concentrations.....	64
6.4.0 tDCS animal model implant viability and stability.....	65
7.0 OVERALL CONCLUSION AND FUTURE PERSPECTIVES .....	66
REFERENCES .....	68

## **1.0 INTRODUCTION**

Transcranial Direct Current Stimulation (tDCS) is a non-pharmacological and non-invasive, low cost therapeutic technique developed as an alternative or complementary method to treat several neuropsychiatric diseases (TORTELLA *et al.*, 2015). tDCS currently makes use of low intensity (0.1 – 2 mA) continuous currents applied directly to the human/animal scalp with the objective of facilitating or hampering neuronal activity in the cortex (NITSCHE *et al.*, 2008) and consequently evoking molecular, cellular and behavioral alterations (FRITSCH *et al.*, 2010). An initial idea is to eliminate the use of intensive pharmacological interventions, in a cost-efficient and low risk manner. Meaning that, patients would be treated with little risk of pharmacological addiction and/or overdose exposure while also lowering overall therapeutic cost (BRUNONI *et al.*, 2012).

The use of transcranial electrical stimulation (tES) to treat diseases is no new feature. Documents dating back to the Roman Empire (27 B.C. – 476 A.D.) describe the use of live electric rays from the Toperdiniformes order put to rest over the human scalp as a method of relieving headaches. Later in the 11th century in Persia, the same method was applied as a possible therapeutic treatment for epilepsy. Moreover, it quickly spread to other countries such as Africa, where they attempted to “Expel demons from one’s body” using electric rays, and Germany, which later developed a frictional crank-controlled electrostatic generator to produce electrical therapeutic currents to treat patients with epilepsy (SARMIENTO *et al.*, 2016).

Despite its long history, tDCS has only recently become a scientific beacon of study. In a quick search in PubMed data bank from the National Center for Biotechnology Information (NCBI) using the key-word “Transcranial Direct Current Stimulation”, one may observe 3849 results excluding reviews. Such numbers are scattered through time, having 1984 to 1989 as its first appearances, 1991 to 1999 an increase in yearly published articles and from 2000 to 2018 a much heavier distribution in publication. The largest portion of these publications aim at assessing and proposing alternative treatments for psychiatric disorders and motor disabilities (search done in October/2018).

Depression has been one of the most studied diseases in terms of tDCS efficiency both in pre-clinical and clinical trials (FREGN *et al.*, 2016). Studies have shown that tDCS diminishes overall depressive symptoms scored through the Hamilton Depression Rating Scale (HDRS) (BRUNONI *et al.*, 2012). Additionally, Boggio *et al.* (2008) tested tDCS’

therapeutic potential in patients with AD. When treated with electrical currents these patients presented a significant improvement in Visual Recognition Memory (VRM) task. Shortly after, they sustained that tDCS increased the accuracy of memory recognition assessed through the Word Recognition Task (WRT) in tDCS-AD patients compared to Sham-AD (non-stimulated AD patients) (BOGGIO *et al.*, 2012).

tDCS has also been shown to improve working memory (BOGGIO *et al.*, 2006) and verbal fluency in patients with Parkinson's Disease (PD) (PEREIRA *et al.*, 2013), motor-evoked potential response time and intensity in stroke victims (BAKER *et al.*, 2010) and presented considerable rescue of swallowing in patients with Multiple Sclerosis (MS) (COSENTINO *et al.*, 2018), among many other studies.

Additionally, tDCS has been extrapolated as a human enhancement tool for ameliorating working memory (FREGN *et al.*, 2005), declarative and nondeclarative memory (NITSCH *et al.*, 2003), hand motor function (BOGGIO *et al.*, 2006) and executive functions.

Yet, guidelines discussing the boundaries of human enhancement and population accessibility to tDCS are not available, therefore, the use of tDCS in such finality is discussed among many researches and at times is considered polemic (LEFAUCHEUR *et al.*, 2017). There have also been contrasting results surrounding tDCS' efficacy in both animals and humans (BRUNONI *et al.*, 2011).

Essentially, tDCS is composed by two wires coupled to electrodes (anode<sup>-</sup> and cathode<sup>+</sup>) and a current generator capable of controlling the output of low intensity currents and its duration (Fig. 1) (MEINZER *et al.*, 2014).

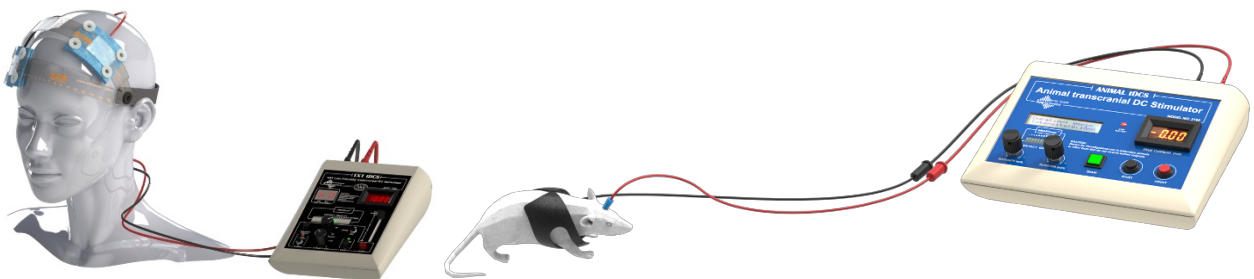


**Figure 1. Human and mouse tDCS layout.** Left figure shows current generator (black) with intensity and duration adjustable controls and displays. Electrode disposition (anode and cathode) over the human scalp. Right figure shows current generator (blue) with intensity and duration adjustable controls and displays. Electrode disposition anode over the mouse's scalp and cathode onto its thorax. Figures adapted from Soterix Medical.

There are currently two forms of tDCS, the anodal, also known as the excitatory stimulation, and the cathodal, known as the inhibitory stimulation (STAGGI *et al.*, 2011). In both methods electrical currents flow from the anode towards the cathode, differing exclusively on electrode positioning over the scalp. In the anodal stimulation (excitatory), the anode is positioned over the area intended to be modulated and the cathode positioned over a reference region which should have little influence in the desired treatment (example: Humans - shoulders chest or supraorbital bone, Mice – ears, thorax and back) while in the cathodal (inhibitory) stimulation the cathode is positioned over the region of interest and the anode over a non-influential region (DASILVA *et al.*, 2011). This disposition reflects directly on how neurons will respond to the weakly applied electrical current (MARQUEZ-RUIZ *et al.*, 2012).

Electric currents applied over the cortical area for both anodal and cathodal stimulation will produce radial (spreading over the cortex parallel to the cellular membranes) and tangential currents (down towards the axonal terminals). These forms of currents might determine what compartments (soma, dendrites, axon and axonal terminals) will be modulated. Current propagation and compartment modulation are correlated to the affected area. Radial currents will evoke a much larger cortical area. The focal point (under the modulatory electrode) will receive an input current and produce an electrical field which will spread over the somatic bodies. While tangential currents will travel parallel to the axons producing synaptic-specific modulation (RAHMAN *et al.*, 2013).

In addition, a different effect (inhibitory or excitatory) may take place depending on the initial affected compartment. Studies have shown that a somatic hyperpolarization is associated to an axonal depolarization and cellular excitation. In contrast, a somatic depolarization is associated to an axonal hyperpolarization and cellular inhibition (PELLETIER *et al.*, 2015). A theory would be placed around an idea of feedback. Due to a hyper or depolarization on the somatic body a cellular response would be an attempt to counter the initial stimuli, producing a  $\text{Ca}^{++}$  dependent opposite effect on the axon and axonal terminals.

The specific cellular and molecular mechanisms that allows such characterizations haven't been fully described (FRITSCH *et al.*, 201). McCaig *et al.* (2000) were able to isolate an exclusive mechanism behind anodal tDCS. The study showed a higher



activation of the tropomyosin-receptor kinase (Trk), a known Brain-Derived Neurotrophic Factor (*BDNF*) receptor (FRITSCH *et al.*, 2010). *BDNF* is a widely expressed protein known to regulate neural circuit development, structure and synaptic plasticity (BRAMHAM *et al.*, 2005).

A further description on how tDCS-*BDNF* modulation works was suggested in pyramidal neurons, a type of cortical and hippocampal neuron capable of secreting glutamate (BECKERS *et al.*, 2011). A higher calcium ( $\text{Ca}^{++}$ ) influx of a modulated neuron (exposed to anodal electrical currents) will evoke higher numbers of neurotransmitter vesicle diffusion. The now released glutamate to the synaptic-gap will bind to the  $\alpha$ -amino-3-hydroxy-5-methyl-4-isoxazolepropionic acid receptor (AMPA) on the post-synaptic membrane. AMPA is an ionic-channel bound protein, which after activation allows sodium ( $\text{Na}^+$ ) fluctuation (KAMPA *et al.*, 2004). Due to a much larger concentration of extracellular  $\text{Na}^+$  a high intracellular influx will be produced leading to membrane potential shifting (KABAKOV *et al.*, 2012) and neuronal depolarization.

In consequence of the action potential shifting by the rise in intracellular  $\text{Na}^+$ , the N-methyl-D-aspartate receptor (NMDAR), a glutamate and action potential dependent (for magnesium ( $\text{Mg}^{++}$ ) removal) ionic-channel will open, allowing a next-step of intracellular influx of  $\text{Na}^+$  and  $\text{Ca}^{++}$  (GIORDANO *et al.*, 2017).  $\text{Na}^+$  will further assist in full membrane depolarization. Once  $\text{Ca}^{++}$  enters the post-synaptic membrane it may follow distinctive paths. Its first path is promoting *BDNF* secretion (resting in synaptic-vesicles) towards the pre-synaptic axonal terminals containing Trk  $\text{Ca}^{++}$  ionic-channel associated receptors and further enhancing glutamate release from the pre to post-synaptic membrane (KAMPA *et al.*, 2004). The second path is also the basis of how tDCS is able to generate plastic neuronal alterations, defined as long-term potentiation (LTP) and long-term depression (LTD) (MARQUEZ-RUIZ *et al.*, 2012).

The  $\text{Ca}^{++}$  influx in the post-synaptic neuron will also mediate transcription factors activation, that are resting over the nuclear-envelope and in the cytoplasmic membrane. This will increase the expression of plasticity genes, evoking alterations such as angiogenesis, microglia activation, *de novo* spiny formation, NMDAR, AMPAR and glutamate availability, glutamate release increase and  $\gamma$ -aminobutyric acid (GABA) neuron activity decrease (Fig. 2). Such effects are anodal stimuli dependent and are

characterized as LTP (STAGGI *et al.*, 2011). The cathodal stimuli present strongly contrasting effects and is characterized as LTD (MARQUEZ-RUIZ *et al.*, 2016). tDCS  $\text{Ca}^{++}$  surges have also been correlated to astrocyte activation and mediation. Through  $\text{Ca}^{++}$  imaging in mice, researchers were able to demonstrate that astrocytes are the first responders after tDCS with neuronal modulation following seconds after (MONAI *et al.*, 2016). The magnitude of these set of effects can be modulated through the adjustment of current intensity, current duration, current density, electrode size, electrode positioning and context (BENNABI *et al.*, 2014).

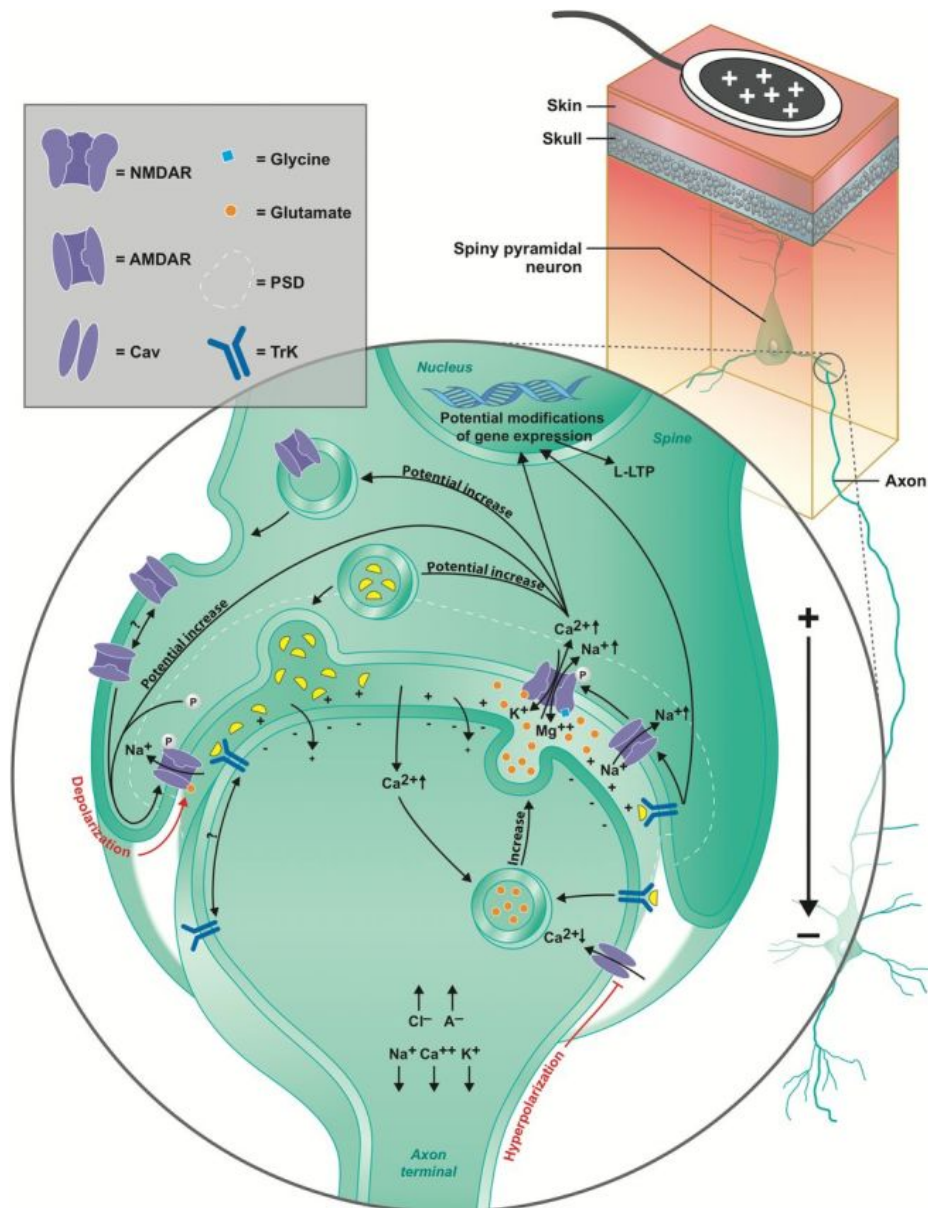


**Figure 2. tDCS underlying mechanism.**

Illustrative figure, showing anodal tDCS theoretical mechanisms. NMDA (N-methyl-D-aspartate receptor), AMPAR ( $\alpha$ -amino-3-hydroxy-5-methyl-4-isoxazolepropionic acid) PSD (post-synaptic density), Cav (Caveolin –  $\text{Ca}^{++}$  channel), TrK (tropomyosin-receptor kinase), Calcium ( $\text{Ca}^{++}$ ), Sodium ( $\text{Na}^+$ ), Magnesium ( $\text{Mg}^{++}$ ). Adapted from Pelletier *et al.* (2015).

Most molecular evidence on tDCS' mechanism and efficiency have been identified within pre-clinical studies. Although human trials have moved forward with little pre-clinical support, many studies have been of great importance for the understanding of tDCS' therapeutic potential and protocol consolidation such as, polarity and timing efficiency (STAGGI *et al.*, 2011). The research showed how cathodal and anodal tDCS evoke contrasting motor explicit learning effects while also determining the importance of task-paired (online) tDCS. The study was carried out in 25 subjects and demonstrated that applying tDCS in humans while they engaged in a specific motor learning task (online tDCS) potentiated performance compared to executing tasks before or after tDCS (offline). There has yet to be studies characterizing specifically how/why online tDCS further improves stimulation effects. A proposed theory is that the electrical current applied through tDCS has the tendency to follow circuits with the least current resistance, hence, current flow will follow circuits with higher neuronal activity in that moment (D'MELLO *et al.*, 2017).

The biggest clinical-molecular contribution of human tDCS trials involves BDNF and the Catechol-O-methyltransferase (COMT), an enzyme responsible for participating in the metabolism of dopamine and other catecholamines (NIERATSCKER *et al.*, 2015). Puri *et al.* (2015) and Stephens *et al.* (2017) demonstrated for both BDNF and COMT, respectively, how polymorphic alterations in these genes have great influence in tDCS' treatment efficiency. The articles associated stimulation efficiency of tDCS-COMT (val/val, val/met and met/met) in different stimulation intensities (1, 1.5 and 2 mA), showing that polymorphism combination and current tDCS greatly influences in working memory gains. While tDCS-BDNF (val/val, val/met and met/met) in different stimulation durations (10-20 min) is associated to the magnitude of evoked neuronal plasticity.

Even though, there has been a great leap in knowledge concerning tDCS in the past 10 years there is still much to be learned in pre-clinical and clinical trials. Due to its

underlying mechanisms, such as plasticity and stimulation potential being in-focused to the brain, and considering the accessibility limitation to the human brain, a quickly executed, safe and validated animal model is considered a necessary step to further study tDCS. Therefore, here we present both a transcranial direct current stimulation mouse model protocol, from surgical procedures, after-care, stimulation and validation (presented in the article below) and additional preliminary results on neurotransmitter dosage, gene expression and behavioral learning evoked alterations through tDCS.

## **2.0 OBJECTIVES**

## **2.1 Overall Objectives**

Produce and validate a fast executing transcranial direct current stimulation mouse model for further molecular and behavioral investigations on tDCS' mechanisms.

### **2.2.0 Specific Objectives**

2.2.1 Develop a fast executing implantable electrode surgical procedure for tDCS.

2.2.2 Determine tDCS' implant stability and time-dependent viability.

2.2.3 Validate gene expression markers for tDCS efficiency.

2.2.4 Investigate molecular and behavioral alterations evoked by tDCS.

### **3.0 PUBLISHED ARTICLE**

## Video Article

# Transcranial Direct Current Stimulation (tDCS) in Mice

Eduardo de Souza Nicolau<sup>1</sup>, Kevin Augusto Farias de Alvarenga<sup>1</sup>, Helia Tenza-Ferrer<sup>1</sup>, Matheus Carvalho Alves Nogueira<sup>1</sup>, Fernanda Donizete Rezende<sup>1</sup>, Nycolle Ferreira Nicolau<sup>1</sup>, M elcar Collodetti<sup>1</sup>, D ebora Marques de Miranda<sup>1</sup>, Luiz Alexandre Viana Magno<sup>1</sup>, Marco Aur elio Romano-Silva<sup>1</sup>

<sup>1</sup>Centro de Tecnologia em Medicina Molecular (CTMM), Faculdade de Medicina, Universidade Federal de Minas Gerais

Correspondence to: Marco Aur elio Romano-Silva at [romano-silva@ufmg.br](mailto:romano-silva@ufmg.br)

URL: <https://www.jove.com/video/58517>

DOI: [doi:10.3791/58517](https://doi.org/10.3791/58517)

Keywords: Transcranial Direct Current Stimulation, tDCS, Animal Model, Electrode Implantation, Molecular Markers, Neurostimulation

Date Published: 9/11/2018

Citation: de Souza Nicolau, E., de Alvarenga, K.A., Tenza-Ferrer, H., Nogueira, M.C., Rezende, F.D., Nicolau, N.F., Collodetti, M., de Miranda, D.M., Magno, L.A., Romano-Silva, M.A. Transcranial Direct Current Stimulation (tDCS) in Mice. *J. Vis. Exp.* (), e58517, doi:10.3791/58517 (2018).

## Abstract

Transcranial direct current stimulation (tDCS) is a non-invasive neuromodulation technique proposed as an alternative or complementary treatment for several neuropsychiatric diseases. The biological effects of tDCS are not fully understood, which is in part explained due to the difficulty in obtaining human brain tissue. This protocol describes a tDCS mouse model that uses a chronically implanted electrode allowing the study of the long-lasting biological effects of tDCS. In this experimental model, tDCS changes the cortical gene expression and offers a prominent contribution to the understanding of the rationale for its therapeutic use.

## Video Link

The video component of this article can be found at <https://www.jove.com/video/58517/>

## Introduction

Transcranial Direct Current Stimulation (tDCS) is a non-invasive, low-cost, therapeutic technique, which focuses on neuronal modulation through the use of low-intensity continuous currents<sup>1</sup>. There are currently two setups (anodal and cathodal) for tDCS. While the anodal stimulation exerts a current electric field too weak to trigger action potentials, electrophysiology studies have shown that this method produces changes in synaptic plasticity<sup>2</sup>. For example, evidence shows that tDCS induces long-term potentiation (LTP) effects such as increased peak amplitude of the excitatory postsynaptic potentials<sup>3,4</sup> and modulation of cortical excitability<sup>5</sup>.

Conversely, cathodal stimulation induces inhibition, resulting in membrane hyperpolarization<sup>6</sup>. A hypothesis for this mechanism is based on the physiological findings where tDCS is described to modulate action potential frequency and duration in the neuronal body<sup>3</sup>. Notably, this effect does not directly evoke action potentials, though it can shift the depolarization threshold and facilitate or hamper neuronal firing<sup>7</sup>. These contrasting effects have been previously demonstrated. For example, anodal and cathodal stimulation produced opposing effects in conditioned responses registered *via* electromyography activity in rabbits<sup>8</sup>. However, studies have also shown that prolonged anodal stimulation sessions may decrease excitability while increasing cathodal currents may lead to excitability, presenting self-contrasting effects<sup>3</sup>.

Both anodal and cathodal stimuli aggregate the use of electrode pairs. For example, in anodal stimulation, the "active" or "anode" electrode is placed over the brain region to be modulated whereas the "reference" or "cathode" electrode is situated over a region where the effect of current is assumed to be insignificant<sup>9</sup>. In the cathodal stimulation, electrode disposition is inverted. The stimulation intensity for effective tDCS depends on the current intensity and electrode dimensions, which affect the electric field differently<sup>10</sup>. In most published studies, the average current intensity is between 0.10 to 2.0 mA and 0.1 mA to 0.8 mA for human and mice, respectively<sup>6,11</sup>. Although the electrode size of 35 cm<sup>2</sup> is typically used in humans, there is no proper understanding regarding electrode dimensions for rodents and a more thorough investigation is needed<sup>6</sup>.

tDCS has been proposed in clinical studies with the attempt of offering an alternative or complementary treatment for several neurological and neuropsychiatric disorders<sup>11</sup> such as epilepsy<sup>12</sup>, bipolar disorder<sup>13</sup>, stroke<sup>5</sup>, major depression<sup>14</sup>, Alzheimer's disease<sup>15</sup>, multiple sclerosis<sup>16</sup> and Parkinson's disease<sup>17</sup>. Despite growing interest in tDCS and its use in clinical trials, detailed cellular and molecular evoked alterations in brain tissue, short and long-lasting effects, as well as behavioral outcomes, are yet to be more deeply investigated<sup>18,19</sup>. Since a direct human approach to thoroughly study tDCS is not viable, the use of a tDCS animal model may offer valuable insights into the cellular and molecular events underlying the therapeutic mechanisms of tDCS due to the accessibility to the animal's brain tissue.

Available evidence is limited regarding tDCS models in mice. Most of the reported models used different implanting layouts, electrode dimensions, and materials. For example, Winkler *et al.* (2017) implanted the head electrode (Ag/AgCl, 4 mm in diameter) filled with saline and fixed it to the cranium with acrylic cement and screws<sup>20</sup>. Different from our approach, their chest electrode was implanted (platinum, 20 x 1.5 mm). Nasehi *et al.* (2017) used a procedure very similar to ours, although the thoracic electrode was made from a saline-soaked sponge (carbon filled, 9.5 cm<sup>2,21</sup>). Another study implanted both electrodes into the animal's head, which was achieved by using fixed plates and covering the



animal's head with a hydrogel conductor<sup>22</sup>. Here, we describe a tDCS mouse model that uses a chronically implanted electrode through simple surgical procedures and tDCS setup (**Figure 1**).

## Protocol

Individually-housed male adult (8-12 weeks) C57BL/6 mice were used in this experiment. Animals received proper care before, during and after experimental procedures with food and water *ad libitum*. All procedures were approved by the animal ethics committee from Federal University of Minas Gerais (*protocol number 59/2014*).

### 1. Electrode Placement

#### 1. Sedating and fixating the animal onto the stereotaxic apparatus

1. Sterilize all the necessary surgical instruments.  
Note. Surgical instruments were sterilized for 3 minutes at 440 °C. Cotton swabs were autoclaved at 20 psi (pounds per square inch) at 121 °C for 20 min.
2. Adjust the thermal platform controller to 37 °C.
3. Weigh the animal and calculate the appropriate dose for anesthesia induction. Use a mixture of ketamine and xylazine at a dose of 100 mg/kg ketamine and 8 mg/kg xylazine, given intraperitoneally (needle size, 31 G). The animal should fall asleep within 2 to 3 min.
4. Use an electric shaver or razor to shave down the surgical site.
5. Place the animal onto the stereotaxic apparatus over the pre-warmed heating plate.
6. Hold the animal's head and insert the tip ear bars into each of the animal's ears to fix it to the stereotaxic platform.
7. Verify there is no lateral head shifting and little vertical movement after by slowly shifting the animal's head positioning.
8. Gently slide the anesthesia mask over the mouse's nose and fix it in place by tightening the screw.
9. Set the isoflurane to 1% with 1.0 L/min of O<sub>2</sub>.
10. Apply eye ointment to the animal's eyes to prevent corneal drying during the surgery.

#### 2. Attaching the implant to the animal's head

1. Use the cotton swabs to prepare the surgical site with three alternating scrubs of povidone-iodine (or 2% chlorhexidine) and 70% ethanol.
2. Use a pair of tweezers to verify anesthesia depth by lightly squeezing the animal's toes and verifying the loss of animal's pedal withdrawal (toe pinch) reflex.
3. Make an incision about 3 mm posterior to the animal's ear line and stop at the eye line. The incision site must have approximately 1 cm in length to be large enough to receive the implant.
4. Gently scrape the cranium with a bone scraper to improve glue and cement adherence. Do this light handedly with the intention of creating micro scratches.
5. Carefully position surgical hooks to the loose skin to maintain an open surgical field and free of obstructions such as skin and fur.
6. Use a sterile cotton swab to dry the animal's scalp.
7. Use a dissecting microscope to visualize the top of the animal's cranium.
8. Attach a needle to the stereotaxic holder and locate the bregma. Position the needle directly above the animal's head slightly touching the bregma.
9. Zero out all coordinates on the digital tracer and then raise the needle.
10. Fix the tDCS implant on the stereotaxic holder. Position the implant over the animal's head and lower it slowly onto the region of interest using the proper stereotaxic coordinates.
11. Use a needle to spread 1 drop (approximately 35  $\mu$ L) of super glue onto the implant's base.
12. Slowly move the holder downwards until it touches the skull. Be sure that the implant base is entirely in contact with the surface.
13. Prepare the surgical cement according to the manufacturer's instructions.
14. After precise positioning, apply 3 thin, even layer of cement across the cranium and onto the lower portion of the implant. Apply drop per drop using an application brush. Layers must form a hill-shaped structure for further structural support of the implant.
15. Leave the implant's screw thread clean of cement to allow a smooth, unobstructed connection.
16. Allow each layer to dry for approximately 4 minutes.
17. When dry, carefully remove the holder until it is completely detached from the implant. Always use extreme caution when handling the implant, since it may be accidentally extracted from the animal's skull.

#### 3. Finishing surgery and post-surgical care

1. Hydrate the animal's skin in the incision site with a saline-soaked cotton swab.
2. Coat the skin over the base of the tDCS implant.
3. Use a pair of tweezers to bring the tissue together and close the incision with a drop of surgical tissue glue per 0.2 cm of tissue.
4. Infiltrate 1-2% lidocaine in the incision site and underlying tissues.
5. Hydrate the mouse with 500  $\mu$ L of lactate Ringer's solution subcutaneously.
6. Place the mouse into a pre-warmed (37 °C) clean, single-housed cage.
7. Put a small dish with wet food pellets in the cage for easy access to food in the following hours.
8. Register the animal's post-surgical weight.
9. Give the animal ketoprofen (5 mg/kg) subcutaneously after the surgery and on the next 2 days.
10. Monitor the recovery of the animal closely for at least 1 week. Assess any sign of distress, such as piloerection, lack of grooming, reduced locomotion, wound scratching and inflammation of the surgical site.

## 2. tDCS Setup and Stimulation

### 1. tDCS Setup (see Figure 2)

Note. Make sure that the tDCS stimulator is fully charged.

1. Attach the anode and cathode cables to the tDCS stimulator and make them available near the stimulation site. Attach the pin-type electrode to the stereotaxic holder.
2. Set the thermal platform to 37 °C.
3. Turn on the oxygen flowmeter on the inhalation anesthesia system to 1 L/min.
4. Place the mouse into the anesthesia induction chamber.
5. Turn on the isoflurane vaporizer to 3%. Allow the animal to undergo isoflurane effects for 4 min.
6. While the animal is in the induction chamber, use a sterile syringe to fill the body electrode with 0.9% saline solution.
7. Remove the animal from the induction chamber and position its chest over the body electrode.
8. Gently slide the anesthesia mask over the mouse's nose and fix it in place. Lower the isoflurane output to 1.5%.
9. Fill the implant and the pin-type electrode with saline and carefully attach them.
10. Adjust stimulation time and current intensity.
11. Verify the contact quality on the tDCS stimulator. Optimal contact goes from 7 to 10 on a 1 to 10 scale.

### 2. Stimulation

1. Start the stimulation.
2. Observe the current ramping up for 30 s to the selected value and maintaining itself steady for the established time, then, at the end of the session ramping down again.
3. Activate the sham button for control mice.
4. Observe the current ramping up for 30 s to the selected value and then down to 1 for the rest of the stimulation period with a final ramp to the selected value at the end with a consecutive ramp down.
5. Once the stimulation session is complete, carefully transfer the animal to a pre-warmed (37 °C) cage for 10 min.  
Note. Animals start to awaken after 3 min.
6. Turn the inhalation anesthesia system off.

## Representative Results

The surgical protocol presented long-term implant stability for at least one month, with no inflammatory signals at the stimulated site nor any other undesired effect. All the animals survived the surgical procedure and tDCS sessions ( $n = 8$ ). In this experiment, tDCS implants were positioned over the M1 and M2 cortices (+1.0 mm anterior-posterior and 0.0 mm lateral to bregma). One week later, tDCS ( $n = 3-4$ ) and sham ( $n = 3$ ) mice were stimulated for five consecutive days during 10 min at 0.35 mA. Contact quality (CQ) values were registered to assess implant viability and no significant differences were found between the groups during a 5-day stimulation procedure (**Figure 3A**). By using this animal model, stimulation success can be determined through the evaluation of gene expression levels for brain-derived neurotrophic factor (*BDNF*) and glial fibrillary acidic protein (*GFAP*). Both *BDNF* and *GFAP* presented significantly higher mRNA levels in the cortex area below the implant when compared to the sham group. The effects of tDCS on gene expression seem to be restricted to specific genes since expression levels of the activity-regulated cytoskeleton-associated protein (*ARC*), and synapsin 1 (*SYN1*) genes were not changed (**Figure 3B**).

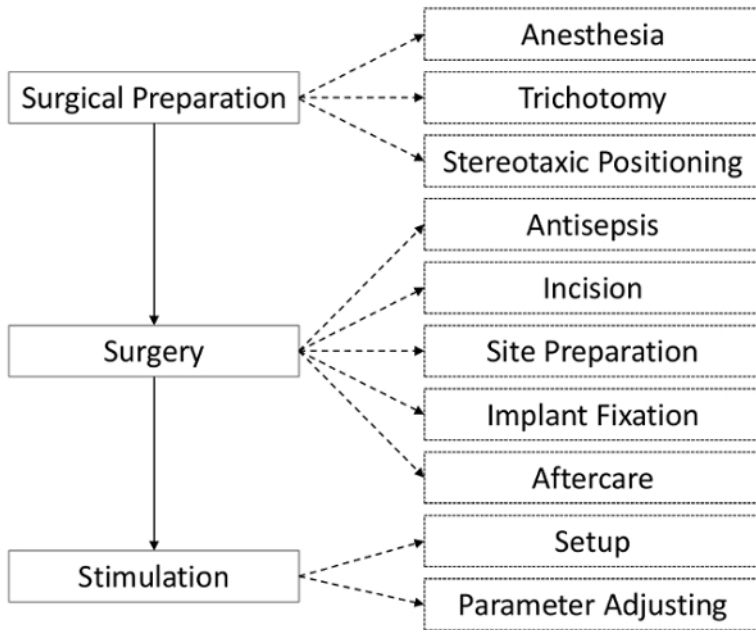


**Figure 1. Experimental steps used for implant surgery and stimulation.** A schematic flowchart of the steps through tDCS implant placement, tDCS setup, and stimulation procedure. [Please click here to view a larger version of this figure.](#)

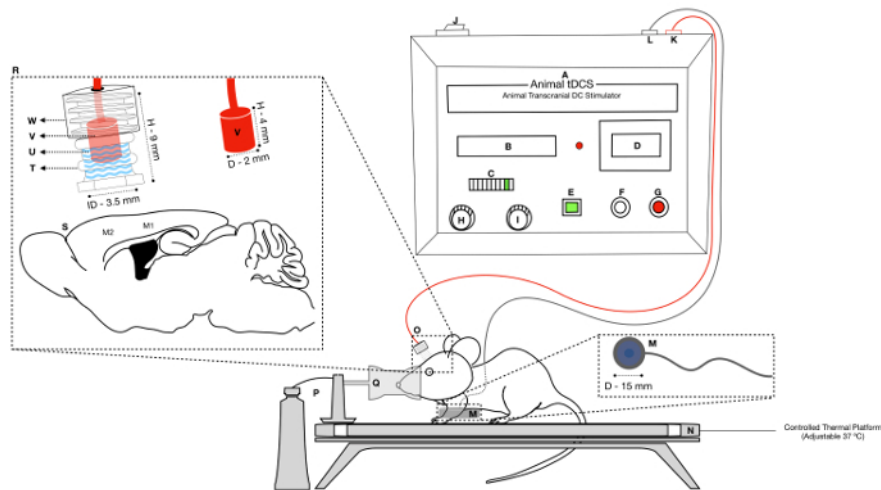


**Figure 2. tDCS Setup.** The right superior image corresponds to a schematic of the tDCS current stimulator (A), which contains a display for the current intensity and stimulation duration (B), a CQ display (C) scaling from 1 to 10 and a true current display (D). The tDCS stimulator also has buttons to activate sham stimulation (E), to start stimulation (F), and to abort the protocol (G). The two knobs are used for adjusting the current intensity (H) and stimulation duration (I). The on/off switch is located at the rear side (J). Two female insertable entrances are utilized for the electrode cables (K, negative pole) (L, positive pole). The right inferior image shows the animal setup with the head electrode made of Ag/AgCl (O) and the body electrode made of nickel-plated brass (M) sets and their respective dimensions. An auto adjusted thermal platform (N) maintains the animal's temperature, and isoflurane mixed with 100% oxygen (P) is supplied through the stereotaxic gas mask (Q). The inset (R) shows the positioning of the anode relative to the cortical motor regions M1 and M2 (S). The tDCS headstage is composed of an implantable holder (T) filled with saline (0.9% NaCl) (U) which is closed with a pin-type electrode (V) attached to a plastic cap (W). The respective dimensions are depicted in millimeters (D = diameter, H = height, ID = internal diameter). [Please click here to view a larger version of this figure.](#)

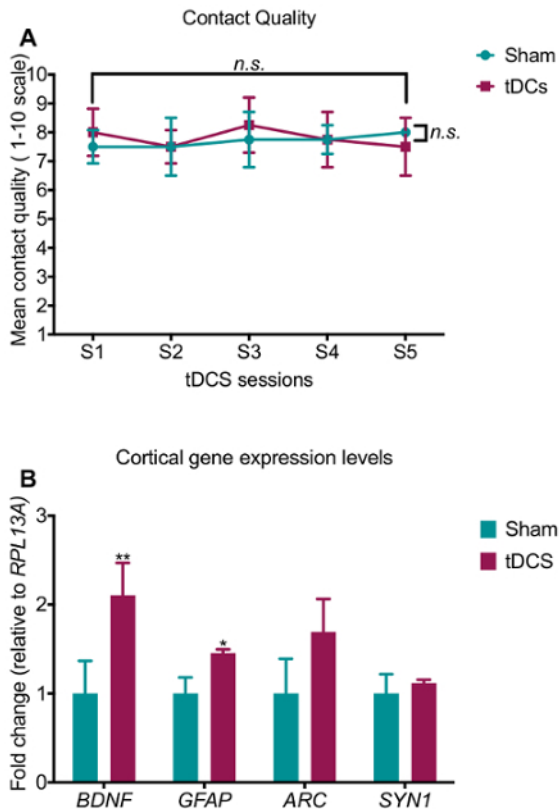


**Figure 3. Contact quality and gene expression changes evoked by tDCS.** (A) No statistical differences were observed for contact quality (CQ) among the groups. Two-way repeated measures ANOVA, treatment *versus* day interaction ( $F_{4,30} = 0.552$ ,  $P = 0.698$ ), treatment factor ( $F_{4,30} = 0.349$ ,  $P = 0.810$ ), day factor ( $F_{1,30} = 0.157$ ,  $P = 0.694$ ). (B) Quantitative polymerase chain reaction gene expression data for *BDNF* (Brain-derived neurotrophic factor), *GFAP* (glial fibrillary acidic protein), *ARC* (activity-regulated cytoskeleton-associated protein) and *SYN1* (synapsin 1). mRNA levels of both *BDNF* ( $p = 0.0081$ ) and *GFAP* ( $p = 0.0108$ ) were increased while no change was detected for *ARC* ( $p = 0.0760$ ) and *SYN1* ( $p = 0.508$ ), according to D'Agostino-Pearson normality test followed by unpaired parametric Student's t-test. Fold changes were calculated using the  $2^{-\Delta\Delta CQ}$  method relative to *RPL13A* gene. In all graphs, tDCS group is magenta and sham group is green;  $n = 3-4$ /group. Data are expressed as mean and  $\pm$  S.E.M. error bars. *n.s.* = nonsignificant,  $p \leq 0.05^*$ ,  $p \leq 0.01^{**}$ . [Please click here to view a larger version of this figure.](#)

## Discussion

In recent years, neurostimulation techniques have been entering clinical practice as a promising procedure to treat neuropsychiatric disorders<sup>23</sup>. To reduce the constraint imposed by the lack of knowledge of the mechanisms of neurostimulation, we presented here a tDCS mouse model carrying an electrode that can target brain regions. Since the electrode is chronically implantable, this animal model enables the investigation of long-lasting biological effects evoked by tDCS (for at least 1 month) in complex stimulation patterns. The described tDCS animal model presents high implant tolerance and little chance of infection if executed correctly. Overall, the surgery steps to place the implant are of quick and straightforward execution (30 min/animal). One additional advantage of this tDCS model is that it is possible to track the electrode contact quality and the actual current stimulation values.

The main drawback of this animal model is the proper implant fixation on the mouse's cranium. During surgery, it is essential to restrict the animal's head in a manner in which no lateral head shifting is possible (the head will only move vertically). This will assure that the animal's scalp is wholly aligned with the implant's base, allowing proper fixation with the dental cement, and higher precision in modulating the intended target area. It is critical to make the incision large enough to receive the implant. A larger cut may be necessary for some tDCS implants. Using two to four surgical hooks made from hypodermic needles will increase the cemented area. However, avoid placing the hooks too close to the animal's eyes to remove any possibility of lesions. Whereas gently scratching the scalp will improve the adhesion of the super-glue and the cement onto the cranium, any residual debris may prevent good implant adherence. Furthermore, when applying the dental cement, prepare the first layer with a higher viscosity, which avoids the cement of running down the animal's skull. Each cement layer must be allowed to dry for at least 4 min because applying cement over wet layers will delay the hardening of the bottom layers and may cause the implant to shift or even fall. From experience, there must be no more than 3 layers of cement around the implant to avoid obstruction of the screw thread. For both the glue and the cement, be sure to maintain their application restricted to the implant's base. Avoid allowing residue to spread within the implant, which will decrease the surface conductivity and lower the tDCS effects.

The implantable electrode used in this procedure was not fabricated in-house but acquired from a medical research company specialized in producing neuromodulation devices. The implants are made out of polypropylene with 9 mm of height and an outer and inner diameter of 5.7 mm and 3.5 mm, respectively. It can hold a total saline volume of 80  $\mu$ L. The superior portion of the implant is prepared with a screw thread to receive a pin-type electrode holder. The pin-type electrode holder's outer body is also made of polypropylene measuring 4 mm high with a 5.3 mm outer

diameter and a 3.75 mm inner diameter. The electrode pin is made from Ag/AgCl, an inert material used due to its non-dissolving properties (**Figure 2**). Since the implant location is a critical factor for effective tDCS, it is essential to select a proper electrode size according to the region of interest. The implant used in this animal model occupies a surface area of 9.61 cm<sup>2</sup>, spreading the electrical field over a 1.75 mm radius from the intended brain coordinate resulting in a 36,3967 μA/cm<sup>2</sup> current density. Possibly, the tDCS stimulus executed in this protocol was mostly directed to the M1 and M2 cortices.

Usually, the electrode configuration varies according to the intended excitatory or inhibitory stimulation effects (anodal versus cathodal). Although currents will always flow out of the anode in the direction of the cathode, by placing the electrode in inverted terminal positions enables different electrophysiology effects. For example, when ions flow from the cathode in the direction of the anode, the procedure is usually defined as a cathodal stimulation<sup>24</sup>. In this experiment, we performed anodal stimulation in which the anode was placed over the M1/M2 cortices, and the cathode was placed down on the animal's thorax. Thus, in our tDCS setup, it is expected that stimulation produces excitatory potentials<sup>25</sup>. The tDCS effect can also be regulated through the changes in current intensity and duration. Most studies in rodents have used currents varying from 0.2 to 1.0 mA. tDCS currents are expected to generate concentrated heat traveling through the electrode. The direct contact of the tDCS electrode to the animal's head must be avoided. The use of conducting mediums stretches the distance between the electrode and the cranium and prevents the harmful effects of local chemical reactions on the biological tissue. It is possible that a high ionic concentration in liquid conduct media may cause gas formation and bubbles resulted from electrolysis<sup>23,24</sup>. However, this is unlikely to have happened in our tDCS model since isotonic saline solution and low current delivery may decrease the chance of such complications<sup>24</sup>. Nevertheless, other conducting media can also be used with similar efficiencies, such as gelatinous and cream-like conductors<sup>24</sup>.

When choosing the tDCS stimulator, it is vital to consider flexible configuration capabilities. For this protocol, we used a stimulator powered by two 9 V alkaline batteries, which render an expected duration of 1 h of stimulation at 0.35 mA. This stimulator possesses a 0.02 to 1 mA current range with a 10 μA resolution, ideal for rodent stimulation. It is critical that the tDCS stimulator is equipped with an actual current indicator and contact quality (CQ) feedback system to verify optimal stimulation conditions. The current indicator assures when the programmed stimulation intensity is being met. In this tDCS model, the most common factor for faulty current is the presence of bubbles in the saline solution. This issue can be indicated by the CQ feedback system, which measures the contact of both electrodes through the conducting medium and the animal's body. The tDCS stimulator used throughout this experiment displays CQ (SMARTscan) values varying from 1 to 10 on a led scale. This scale is based on voltage values that can infer resistance according to Ohm's law. Led 1 indicates little or atypical low resistance, led 2 indicates open circuit and led 3 through 10 indicates poor to optimal quality (**Figure 2-item C**). The CQ was registered daily for both tDCS and sham groups to verify the electrode viability. It is noteworthy that the average CQ value during stimulation session was higher than 7, meaning that desired currents are being delivered. Overall, no statistical differences were observed for CQ among the groups or day of stimulation (**Figure 3A**). To further validate our tDCS model, we performed quantitative polymerase chain reactions (qPCR) to investigate whether five tDCS sessions (10 min, 350 μA) change cortical gene expression. We found that mRNA levels of *BDNF* and *GFAP* were increased in the M1/M2 cortex of tDCS groups, relative to the Sham mice (**Figure 3B**). These results are consistent with other studies<sup>19,25</sup>.

Neurostimulation studies in experimental animals can provide new insights regarding the brain mechanisms with relevance to neuropsychiatric disorders. Depending on the experimental configuration, the tDCS assembly in this animal model can also be combined with an existing optogenetic or electrophysiology headstage to produce a setup for simultaneous recording and stimulation, alongside a multitude of brain sample experiments. These approaches would be challenging to carry out in humans. Therefore, the opportunity of inserting flexible additions to the currently reported animal tDCS offers a prominent contribution for the understanding of the neural substrates of tDCS and the rationale for its therapeutic use.

## Disclosures

None

## Acknowledgements

We thank Mr. Rodrigo de Souza for assistance in maintaining mouse colonies. L.A.V.M is a CAPES postdoctoral fellow. This work was supported by the grant PRONEX (FAPEMIG: APQ-00476-14).

## References

1. Filmer, H.L., Dux, P.E., Mattingley, J.B. Applications of transcranial direct current stimulation for understanding brain function. *Trends in Neurosciences*. **37** (12), 742-753 (2014).
2. Nitsche, M.A., Paulus, W. Sustained excitability elevations induced by transcranial DC motor cortex stimulation in humans. *Neurology*. **57** (10), 1899-1901 (2001).
3. Kronberg, G., Bridi, M., Abel, T., Bikson, M., Parra, L.C. Direct Current Stimulation Modulates LTP and LTD: Activity Dependence and Dendritic Effects. *Brain Stimulation*. **10** (1), 51-58 (2017).
4. Pelletier, S.J., Cicchetti, F. Cellular and Molecular Mechanisms of Action of Transcranial Direct Current Stimulation: Evidence from In Vitro and In Vivo Models. *International Journal of Neuropsychopharmacology*. **18** (2), pyu047-pyu047 (2015).
5. Chang, M.C., Kim, D.Y., Park, D.H. Enhancement of cortical excitability and lower limb motor function in patients with stroke by transcranial direct current stimulation. *Brain Stimulation*. **8** (3), 561-566 (2015).
6. Lefaucheur, J.P. *et al.* Evidence-based guidelines on the therapeutic use of transcranial direct current stimulation (tDCS). *Clinical Neurophysiology*. **128** (1), 56-92 (2017).
7. Monai, H. *et al.* Calcium imaging reveals glial involvement in transcranial direct current stimulation-induced plasticity in mouse brain. *Nature Communications*. **7**, 11100 (2016).

8. Marquez-Ruiz, J. et al. Transcranial direct-current stimulation modulates synaptic mechanisms involved in associative learning in behaving rabbits. *Proc. Natl. Acad. Sci.* 109, 6710-6715 (2012).
9. Jackson, M.P. et al. Animal models of transcranial direct current stimulation: Methods and mechanisms. *Clinical Neurophysiology*. **127** (11), 3425-3454 (2016).
10. Cambiaghi, M. et al. Brain transcranial direct current stimulation modulates motor excitability in mice. *The European journal of neuroscience*. **31** (4), 704-9 (2010).
11. Monte-Silva, K. et al. Induction of late LTP-like plasticity in the human motor cortex by repeated non-invasive brain stimulation. *Brain Stimulation*. **6** (3), 424-432 (2013).
12. San-Juan, D. et al. Transcranial Direct Current Stimulation in Mesial Temporal Lobe Epilepsy and Hippocampal Sclerosis. *Brain Stimulation*. **10** (1), 28-35 (2017).
13. Brunoni, A.R. et al. Transcranial direct current stimulation (tDCS) in unipolar vs. bipolar depressive disorder. *Progress in Neuro-Psychopharmacology and Biological Psychiatry*. **35** (1), 96-101 (2011).
14. Brunoni, A.R. et al. Trial of Electrical Direct-Current Therapy versus Escitalopram for Depression. *New England Journal of Medicine*. **376** (26), 2523-2533 (2017).
15. Boggio, P.S. et al. Prolonged visual memory enhancement after direct current stimulation in Alzheimer's disease. *Brain Stimulation*. **5** (3), 223-230 (2012).
16. Cosentino, G. et al. Anodal tDCS of the swallowing motor cortex for treatment of dysphagia in multiple sclerosis: a pilot open-label study. *Neurological Sciences*. 7-9 (2018).
17. Kaski, D., Dominguez, R.O., Allum, J.H., Islam, A.F., Bronstein, A.M. Combining physical training with transcranial direct current stimulation to improve gait in Parkinson's disease: A pilot randomized controlled study. *Clinical Rehabilitation*. **28** (11), 1115-1124 (2014).
18. Monai, H. et al. Calcium imaging reveals glial involvement in transcranial direct current stimulation-induced plasticity in mouse brain. *Nature Communications*. **7**, 11100 (2016).
19. Fritsch, B. et al. Direct current stimulation promotes BDNF-dependent synaptic plasticity: potential implications for motor learning. *Neuron*. **66** (2), 198-204 (2010).
20. Winkler, C. et al. Sensory and Motor Systems Anodal Transcranial Direct Current Stimulation Enhances Survival and Integration of Dopaminergic Cell Transplants in a Rat Parkinson Model. *New Research*. **4** (5), 17-63 (2017).
21. Nasehi, M., Khani-Abyaneh, M., Ebrahimi-Ghiri, M., Zarrindast, M.R. The effect of left frontal transcranial direct-current stimulation on propranolol-induced fear memory acquisition and consolidation deficits. *Behavioural Brain Research*. **331** (May), 76-83 (2017).
22. Souza, A. et al. Neurobiological mechanisms of antiallodynic effect of transcranial direct current stimulation (tDCS) in a mice model of neuropathic pain. *Brain Research*. **1682**, (14-23) (2018).
23. Woods, A.J. et al. A technical guide to tDCS, and related non-invasive brain stimulation tools. *Clinical Neurophysiology*. **127** (2), 1031-1048 (2016).
24. Cogan, S.F. et al. Tissue damage thresholds during therapeutic electrical stimulation. *Journal of Neural Engineering*. **13** 2 (2017).
25. Podda, M.V. et al. Anodal transcranial direct current stimulation boosts synaptic plasticity and memory in mice via epigenetic regulation of Bdnf expression. *Scientific reports*. **6** (October 2015), 22180 (2016).

## **4.0 MATERIALS AND METHODS**



#### 4.1.0 tDCS procedures and groups.

All surgical and stimulation procedures may be found in the article above, therefore, they will not be thoroughly discussed here.

8-week-old C57B/L6 male mice were housed individually after surgical tDCS implantation and received proper care in all experimental stages. Food and water were made constantly available. Procedures were approved by the animal ethics and committee from the Federal University of Minas Gerais (*protocol number 59/2014*).

A total of 36 animals underwent surgical and stimulation procedures. Four experimental groups were created, and animals were distributed accordingly:

5/1 Group –  $n = 8$ : Animals in this group received 5 days of anodal stimulation (1 stimulation/day) for 10 minutes at a current intensity of 350  $\mu\text{A}$  and had their tissue collected for gene expression analysis and glutamate dosage 24 hours after the last stimulation session. Obs: Results from this group were also used to develop the tDCS validation article above (Fig. 3).

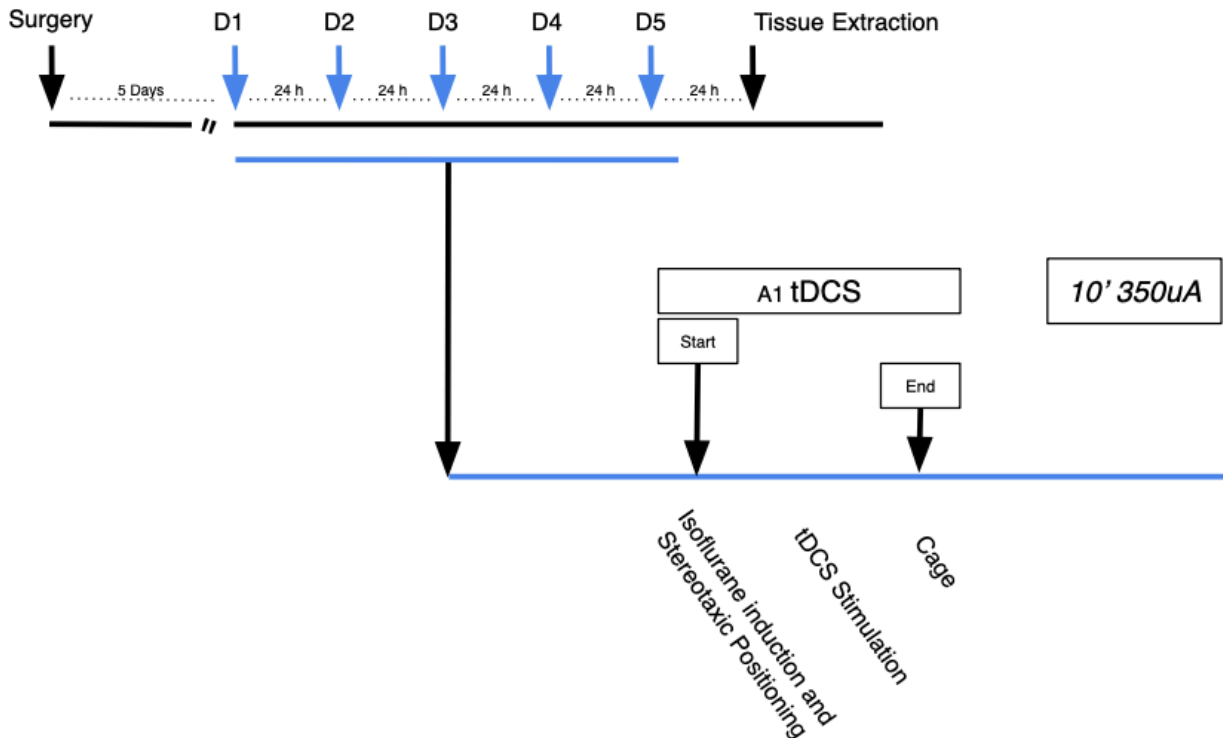




**Figure 3. Experimental timeline of group 5/1.**

Experimental time line of group 5/1, showing surgery (first black arrow from left to right) followed by a 5-day recovery (dotted line) and 5 days of stimulation (blue arrows) with 1 stimulation session per day for 10 minutes at 350 (inferior blue line) and 24 hours of delay between each one. Last black arrow indicating tissue extraction 24 hours after last stimulation session.

5/5 Group –  $n = 8$ : Animals in this group received 5 days of anodal stimulation (1 stimulation/day) for 10 minutes at a current intensity of 350  $\mu\text{A}$  and had their tissue collected for gene expression analysis and glutamate dosage 5 days after the last stimulation session (Fig. 4).

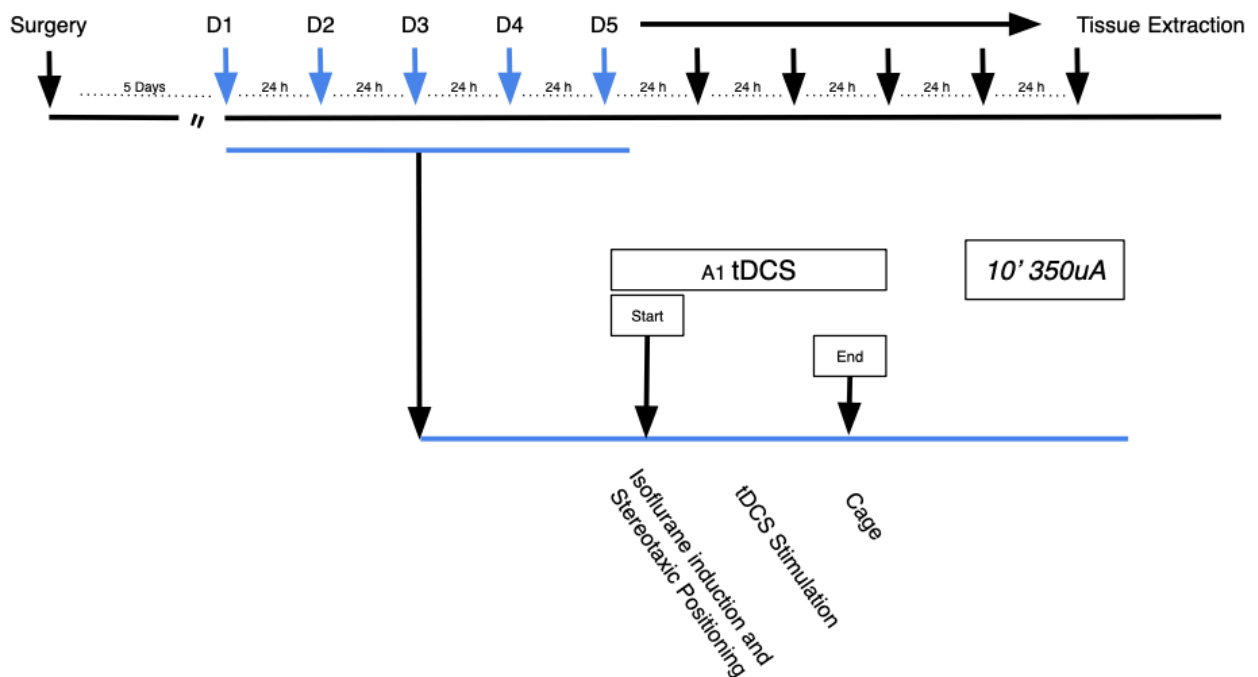


**Figure 4. Experimental timeline of group 5/5.**

Experimental time line of group 5/5, showing surgery (first black arrow from left to right) followed by a 5-day recovery (dotted line) and 5 days of stimulation (blue arrows) with 1 stimulation session per day for 10 minutes at 350 (inferior blue line) and 24 hours of delay (dotted lines) between each one. After stimulation, 4 black arrows indicating waiting period up to tissue extraction (last black arrow), resulting in a final 5-day count.

10/1 Group –  $n = 8$ : Animals in this group received 10 days of anodal stimulation (1 stimulation/day) for 10 minutes at a current intensity of 350  $\mu\text{A}$  and had their tissue

collected for gene expression analysis and glutamate dosage 24 hours (h) after the last stimulation session (Fig. 5).

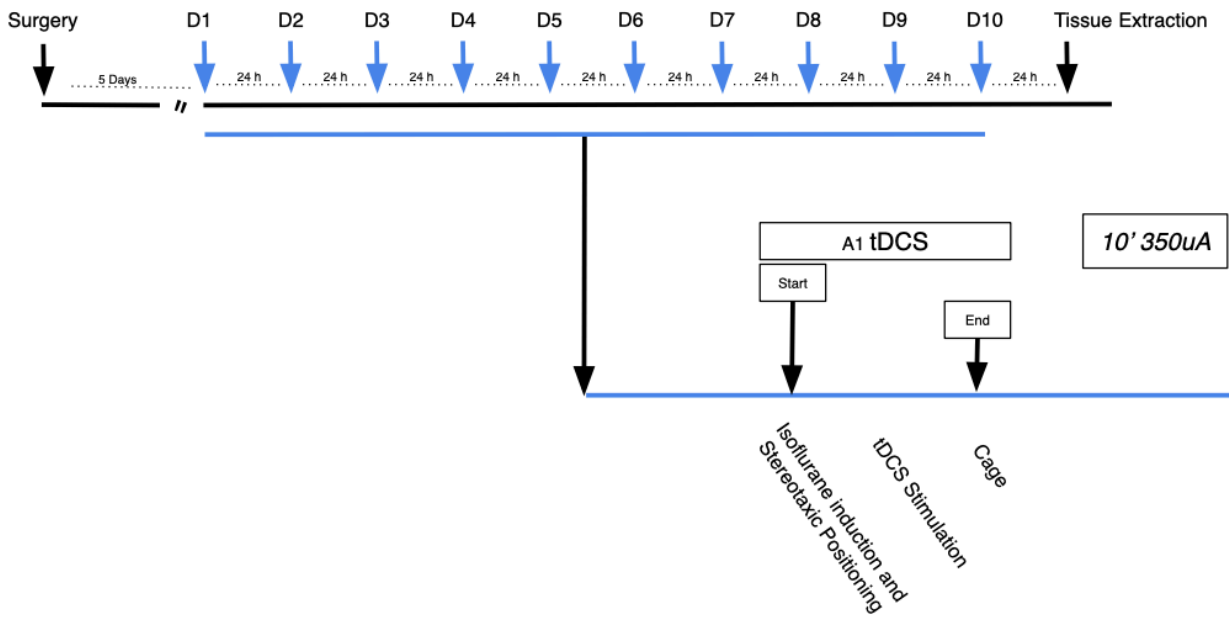


**Figure 5. Experimental timeline of group 10/1.**

Experimental time line of group 10/1, showing surgery (first black arrow from left to right) followed by a 5-day recovery (dotted line) and 10 days of stimulation (blue arrows) with 1 stimulation session per day for 10 minutes at 350 (inferior blue line) and 24 hours of delay (dotted lines) between each one. Last black arrow indicating tissue extraction 24 hours after last stimulation session.

Task Paired Group –  $n = 12$ : Animals in this group underwent a 5-day (3 sessions/day) learning task (Barnes Maze), 20 minutes after the last daily task session animals received anodal stimulation (1 stimulation/day) for 10 minutes at a current intensity of 350  $\mu$ A. Posteriorly, animals had their tissue collected for gene expression analysis and glutamate dosage 24 hours (h) after the last task session. Obs: The task performance was analyzed to further investigate enhancement alterations (Fig. 6).

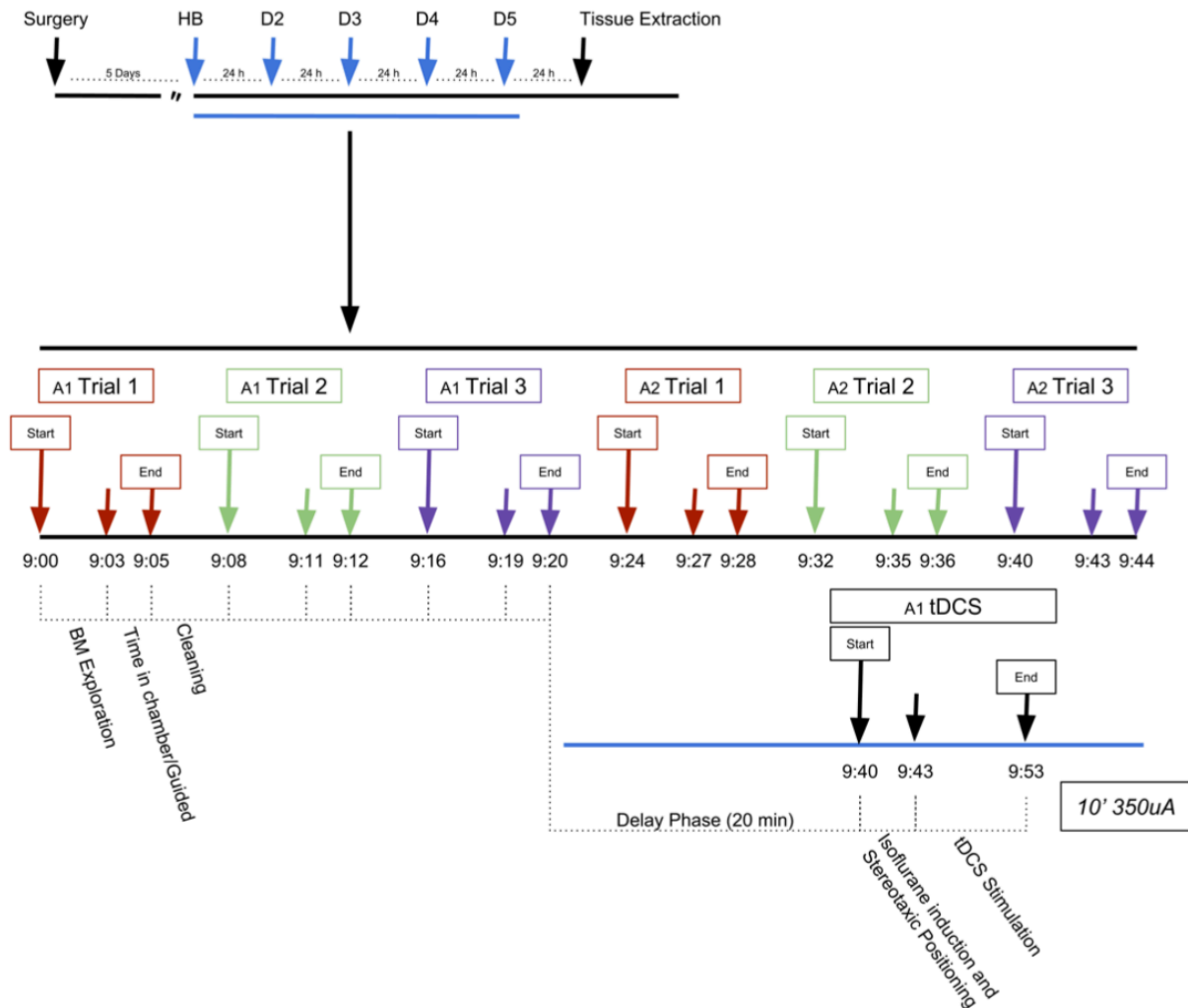


**Figure 6. Experimental timeline of group task-paired.**

Experimental time line of Task-Paired group. Surgery (first black arrow from left to right) followed by a 5-day recovery (dotted line) and 5 days of stimulation (blue arrows) with 1 stimulation session per day for 10 minutes at 350 (inferior blue line) and 24 hours of delay (dotted lines) between each one. Inferior timeline illustrates task performance execution for two animals. First sequence of red, green and purple boxes indicates trails 1, 2 and 3 for animal 1 (A1) and second sequence for animal 2 (A2). Times (starting at 9:00) and ending at (9:44) are representative of execution duration for each trial, composing of BM exploration (animal explores the apparatus) for 3 minutes, time in chamber/guided, animal enters or is guided into the chamber and rests there for 2 minutes and cleaning, the animal is removed and put back in his cage for 3 minutes while the apparatus is cleaned. An additional 20-minute delay phase is presented, showing the interval between the last task session and stimulation.

Each group was divided by two and separated into tDCS (Stimulated group) and Sham (Control Group). For stimulation, the head electrodes (anode) were implanted 1 mm

anterior to the bregma directly onto the skull's midline. The reference electrode (cathode) was placed onto the animal's thorax only when stimulation took place. After surgical procedures animals were individually housed and had no further contact with other animals. In general groups received 0.35 mA of anodal current stimulation for 10 minutes differing on experimental timing and tissue collecting only. For both electrodes saline solution (NaCl – 0.9%) was used as a conducting medium. Group 5/1 and 5/5 tested the possibility of evoking molecular changes in a persistence dependent manner while group 5/1 and 10/1 tested the chronicity dependence. The task-paired stimulated group tested whether tDCS could accelerate and enhance learning process while also providing a molecular profile.

#### **4.2.0 Cervical Dislocation.**

After stimulation procedures animals underwent euthanasia through cervical dislocation following the most humane protocol possible. The initial procedure consisted of pinning the animal's neck (at the base of the skull) with a pair of stiff tweezers, pins or pens, securing the animals tail at its base and simultaneously pushing forward or pulling back one of the extremities to create a dislocation force and consequently immediate death. CO<sub>2</sub> was not considered here since most investigated brain genes present low expression levels and high sensibility to alterations, therefore to guarantee consistent results cervical dislocation was selected as a faster and less stressful procedure.

#### **4.3.0 Tissue extraction and separation.**

After dead, animal's brains were removed and separated into two hemispheres (left and right). Hemispheres were further dissected to separate the motor cortex 1 (M1) and motor cortex 2 (M2). Dissection happened over an ice-cold stainless-steel block for tissue preservation. All tissues were collected into separate 1,5 Eppendorf tubes and immediately put into dry ice. After collection, tubes were stocked at -80°C up to use. Half of the collected left and right hemisphere tissue were directed to gene expression analysis, while the remaining left and right materials were directed to glutamate determination.

#### **4.4.0 Ribonucleic acid (RNA) Extraction and Complementary Deoxyribonucleic acid (cDNA) synthesis.**

RNA was extracted through the ready-to-use TRIzol® (Sigma – Catalog: 15596026) method, which consisted in isolating RNA from cells by maintain RNA integrity and at the same time promoting cellular degradation. A further addition of 99.5% pure chloroform (Merck – Catalog: 1.02445.1000) to the solution allowed the separation of RNA from protein products and DNA after a 20-minute centrifugation at 10.000 rotations per minute (RPM). After centrifugation each component was found in a different compartment of the tube. The RNA layer was collected followed by isopropyl alcohol (Merck – Catalog: 1.09634.1000) precipitation and purification using alcohol 95.0%, 85% and 70% (Anidrol – Catalog: A-1213). RNAs were then submitted to cDNA synthesis using a High-Capacity cDNA Reverse Transcription Kit (ThermoFisher – Catalog: 4368814), consisting of general reverse transcription of all RNA material present in the provided sample.

#### **4.5.0 Quantitative Real Time Polymerase Chain Reaction (qPCR).**

Gene expression was assessed through the cDNA qPCR CFX96 Bio-Rad method and equipment. Plates (Catalog: HSP9601), adhesives (Catalog: MSB1001) and reagents (SYBR™ Green Catalog: 1725271) were acquired from Bio-Rad. A total of 10 genes were selected and analyzed. Genes were chosen according to their protein function which required having neuronal functions such as neuronal and synaptic activity, proliferation, differentiation, plasticity or serve as specific type of neuron marker such as glutamatergic and GABAergic neurons, astrocytes. All primers were constructed on the online NCBI Primer-Blast Tool under the criteria of being specific for the C57B/L6 mouse lineage, not having more than a 500-base pair (pb) product and obligatorily spanning on exon-exon junctions. Primers were synthesized by Integrated DNA Technologies (IDT) in accordance to the requested sequences (Table 1).

Gene	Function	Primer F (5' → 3')	Primer R (3' → 5')	AT (°C)	NC
<b>BDNF</b>	Neuronal growth, differentiation and survival.	CAAAGGATCGGGCGTGCAAAT	ACCTGGTGGACCATTGTGGC	64	50
<b>GFAP</b>	Astrocyte's hallmark.	GGCGAAGAAAACCGCATCAC	ACACCTCACATCACCACGTC	61	40
<b>cFos</b>	Neuronal proliferation and differentiation.	TCTGTCCGTCTCTAGTGCCA	GATCTGTCTCCGCTTGGAGT	64	50
<b>ARC</b>	Synaptic strength regulation.	TTGGTAAGTGCCGAGCTGAG	CGGTAGAAGACCTCCCTCCA	61	40
<b>Gria1</b>	Excitatory neurotransmitter receptor.	AGTCTGCAGAACCGTCTGTG	GCTCAGAGCACTGGTCTTGT	61	40
<b>GAD67</b>	Cortical GABA synthesis.	TACTCCTGTGACAGAGCCGA	TCATACGTTGTAGGGCGCAG	61	40
<b>CAMKIIa</b>	Induction of synaptic potentiation in glutamatergic neurons.	AGCCCTAGTTCCCAGCCTAA	CCCCACCAGTAACCAGATCG	61	40
<b>PSD95</b>	Synaptic strength regulation.	AGCCCCAGGATATGTGAACG	ATGGAACCCGCCTCTTTGAG	61	40
<b>CDK5</b>	Neuron migration, outgrowth and support, and synaptogenesis.	GGGACCTGTTGCAGAACCTAT	ACTGGGGTTCAGAGAGCCTA	61	40
<b>SYN1</b>	Synaptic Activity	CAGAAACCCAGCCAGGATGT	GGAGGGGCTGGCTTTGAG	61	40
<b>RPL13A</b>	Ribosomal protein coding.	GAGGGGCAGGTTCTGGTATTG	GGGGTTGGTATTATCCGCT	60 - 65	40-50

**Table 1. Genes and primers used for qPCR.**

Table showing primers' Forward (5' → 3') and Reverse (3' → 5') sequences with respective annealing temperatures (AT °C) and experimental number of cycles (NC).

The overall procedure consisted of determining how many Quantitation Cycles (Cq) are necessary for each sample to achieve a minimal detectable fluorescence (SYBR™ Green), considering that in each cycle the gene under analysis (primer specific) multiplied exponentially, therefore, samples that achieved an early detectable fluorescence had a higher gene-specific RNA concentration, but only after normalization and statistical analysis, increased or decreased genetic expression was confirmed.

All genetic expression was analyzed through the  $2^{-\Delta\Delta Cq}$  method. Where,  $\Delta^1$  consisted in determining the quantitation cycle (Cq) variation between the target and the RPL13A (housekeeping) gene and  $\Delta^2$  the variation between the normalized Cq of the target genes of the tested samples by the normalized Cq values of the control samples, while the 2 refers to its exponential amplification.

#### 4.6.0 Barnes Maze (Behavioral Assessment).

For the task-paired tDCS group, animals were submitted to a 5-day learning process (Barnes Maze Task). The test consisted in placing animals over a round

apparatus containing 19 false escape holes and one true escape hole (escape chamber) and testing their learning skills by teaching them how to escape from the apparatus. As visual cues, 4 differently shaped images were positioned around the apparatus in all 4 cardinal points. To further motivate the animal to escape a fan was positioned over the apparatus creating an aversive air wave (Fig. 7).

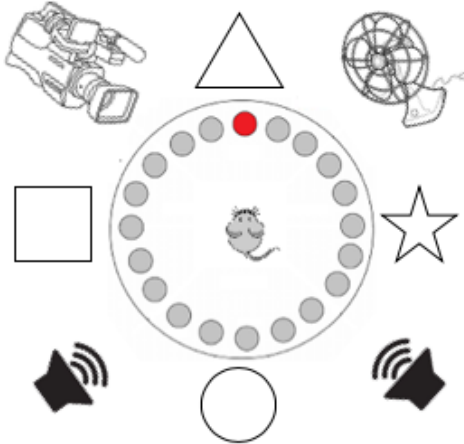


**Figure 7. Illustration of the Barnes Maze apparatus.**

Illustration showing the Barnes maze apparatus disposition. Central peace with a total of 20 holes, 19 false holes (gray) and one escape hole (red). To the right, a fan for generating air flux and to the left, a recording cam. At the bottom, 2 stereo speakers to generate non-aversive white noise.

The test was separated into 2 portions (habituation and training). Animals underwent a 1-day habituation for overall apparatus reconnaissance followed by 4 days of training. During habituation the mice were positioned in the middle of the round platform and were allowed to explore the apparatus freely for 2 minutes. After exploration they were put into the apparatus chamber for another minute. In the next four days animals were submitted to the apparatus and allowed to explore for 3 minutes, after this period if they had yet to escape, animals were slowly guided into the chamber and allowed to stay there for 1 minute. Animals underwent this process 3 consecutive times/day with a 3-minute interval between each trial. After the final session of each day animals rested for 20 minutes followed by 10 minutes of tDCS at a current of 350  $\mu$ A.

Video imaging was recorded during habituation and each trial using the Debut Video Capture (NHC Software) software. Behavioral quantification was done on the AnyMaze (Stoelting Corp.) software to determine number of primary errors (number of wrongly investigated holes before finding the correct escape hole) primary latency (time until the animal finds the correct escape hole) primary distance (distance traveled until the correct escape hole is found) as well for the total number of total errors, latency, distance traveled and mean speed (primary values + values until the animal enters the escape hole – “executes the task”). As each animal performed the task three 3x per day, the analysis was done by acquiring the daily mean of each animal in all 3 trials and then calculating the mean of each group per day. Search strategies assessed. A total of three strategies were considered: Random – animals explore the apparatus randomly to find the escape hole, Serial – animals explore the holes in an outer border sequence to find the escape hole and direct, animals use cued visual signs to locate the hole.

Since the behavioral room was different from the colony room in which animals resided during their entire life, to eliminate the new environment anxiety all animals were exposed to the room for 2 hours before each day of habituation and training.

#### **4.7.0 Total Glutamate determination.**

Total glutamate determination was done through a redox reaction and quantified in the Spectrofluorometer (SHIMADZU – RF-5301 PC). Tissue were homogenized in 0,5 mL of a 7.4 pH Krebs-Ringer-Hepes (KRH) buffer solution to maintain neurotransmitter integrity. KRH Prep: NaCl (116 mM), KCl (4 mM), MgCl<sub>2</sub>.6H<sub>2</sub>O (1 mM), CaCl<sub>2</sub>.2H<sub>2</sub>O (1,8 mM), Glucose (mM) and Hepes Acid (10 mM).

In sequence 15 µL of the homogenized samples were added to a curvet containing 1980 µL of KRH solution with β-Nicotinamide adenine dinucleotide phosphate (NADP – 0.4M) (Sigma – Catalog: N6505-25MG) and Glutamate Dehydrogenase (GDH – 50U) (Sigma – Catalog: G2626). The reaction consisted of indirectly quantifying glutamate through a quantification of the reduction of NADP to NADPH mediated through GDH, that removes hydrogen from glutamate and transferring it to NADP. NADP under an excitation of 260 nanometers (nm) will respond by emitting a 340 nm spectrum, while NADPH will



exclusively respond under an excitation of 340 nm and respond by emitting waves around 450 nm, therefore by quantifying the 450 nm wave emission total glutamate concentration was indirectly determined. At the end of each quantification standard glutamate (1 nm/ol $\mu$ L) was added to the reaction as a relative reference calculator.

Each step consisted in adding the specific reagents and allowing the equipment to stabilize readings as seen in figure 8 (Fig. 8).

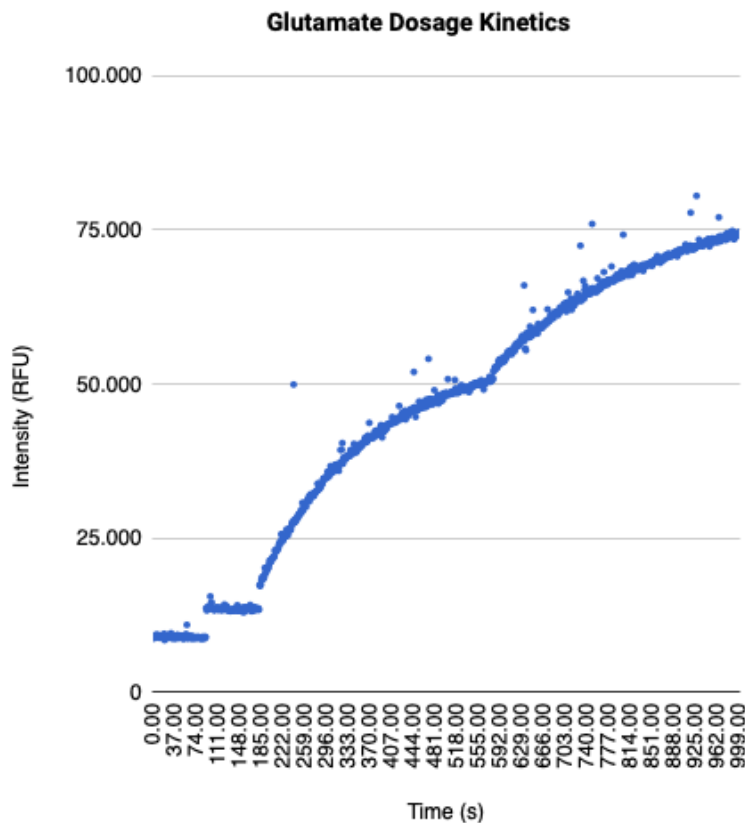


**Figure 8. Illustration of glutamate kinetics for total quantification.**

Illustration showing glutamate dosage kinetics. Initial reading of KRH+NADP (0-90 seconds), addition of GDH (90-180 seconds), addition of sample (180-580 seconds) and standard glutamate (580-999 seconds). RFU (Relative Florescent Units).

Furthermore,  $\Delta$  (variations) were calculated for each step subtracting the final RFU from each stage by the initial RFU of the previous stage. Relative values of glutamate (nmol/ $\mu$ L) for each sample were normalized by total protein concentration using the Bradford Protein Assay (Sigma – Catalog: B6916-500mL) on the VICTOR™ X4 (PerkinElmer 2030).

## **5.0 RESULTS**

Results concerning the tDCS animal model development and validation may be found in the article above, therefore will not be cited here. Moreover, the results presented below refer to the investigation of additional molecular and behavioral alterations evoked by tDCS.

### 5.1.0 tDCS gene expression profile.

tDCS has been strongly tested for gene alteration. Its basic machinery has been theorized to be molecularly bound. Furtherly, there has been evidence that tDCS is able to alter genetic expression especially around BDNF and plasticity changes in the brain. Hence, our first tested hypothesis went around molecular profiling of tDCS under different stimulation protocols.

A total of 10 genes were tested (see materials and methods for gene expression): *BDNF* (Brain-derived neurotrophic factor), *GFAP* (glial fibrillary acidic protein), *cFos* (Fos proto-oncogene), *ARC* (activity-regulated cytoskeleton-associated protein), *Gria1* (glutamate Receptor AMPA 1), *GAD67* (Glutamate Descarboxylase 1), *CAMKII $\alpha$*  (calcium/calmodulin-dependent protein kinase II alpha), *PSD95* (discs large MAGUK scaffold protein 4), *CDK5* (cyclin-dependent kinase 5) and *SYN1* (synapsin 1).

For this we used 3 of the 4 previously described groups (5/1, 5/5 and 10/1) testing stimulated vs. non-stimulated (Sham/Control) groups. Among these, cortical M1/M2 regions were transcranially stimulated for 10 minutes under currents of 350  $\mu$ A.

Group 5/1 focused on presenting initial molecular alterations. As seen in figure 8, expression for *BDNF* and *GFAP* presented higher expression levels for the stimulated group compared to sham. A mild increase tendency for *ARC* and *CAMKII $\alpha$*  may be seen but no statistical differences were detected. *cFos*, *Gria1*, *GAD67*, *PSD95*, *CDK5* and *SYN1* presented highly similar gene expression to the control group (Fig. 9).

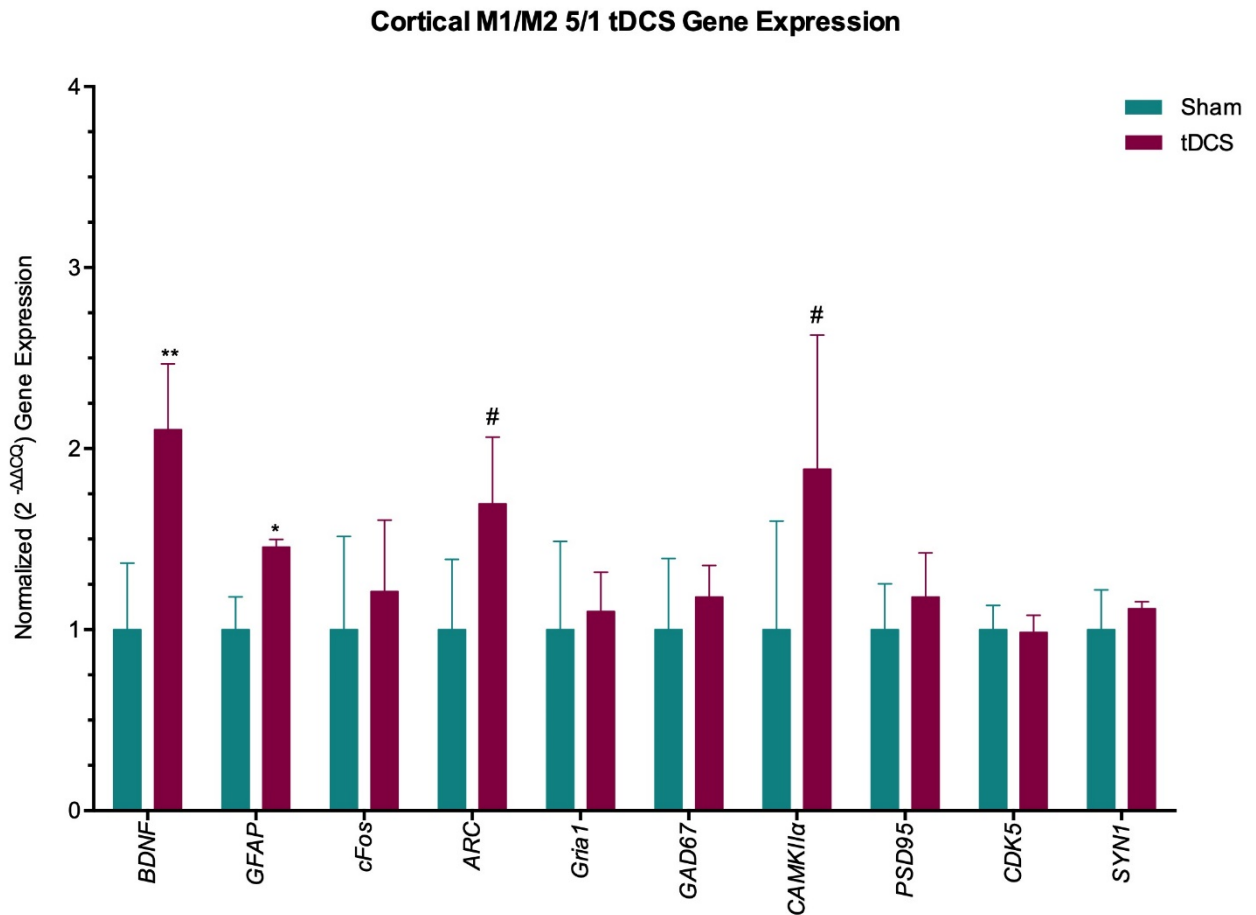


**Figure 9. Gene expression changes evoked by tDCS in group 5/1.**

Quantitative polymerase chain reaction gene expression. tDCS (Magenta/ $n=4$ ) vs. Sham (Green/ $n=4$ ). Stimulated group received currents 10 minutes of 350  $\mu$ A for 5 days (1 sessions/day). Tissue for gene expression collected 1 day after last stimulation. Data for mRNA levels shows *BDNF* ( $p = 0.0081$ ), *GFAP* ( $p = 0.0108$ ), *cFos* ( $p = 0.8557$ ), *ARC* ( $p = 0.0760$ ), *Gria1* ( $p = 0.8404$ ), *GAD67* ( $p = 0.7364$ ), *CAMKII $\alpha$*  ( $p = 0.0679$ ), *PSD95* ( $p = 0.4640$ ), *CDK5* ( $p = 0.7367$ ) and *SYN1* ( $p = 0.5089$ ) (from left to right). Groups were tested for normality under the D'Agostino-Pearson test followed by unpaired parametric Student's t-test to determine differences between means. Gene expression changes were calculated using the  $2^{-\Delta\Delta CQ}$  method relative to *RPL13A* gene. Data are expressed as mean and  $\pm$  S.E.M. error bars. *n.s.* = nonsignificant, # = strong tendency ( $p \leq 0.05 - \geq 0.10$ ),  $p \leq 0.05^*$ ,  $p \leq 0.01^{**}$ .

After initial results molecular evoked alterations were tested for persistency with the 5/5 group, under the supposition that 5 days of tDCS would evoke expression alterations for up to 5 days after the last stimulation session. None of the gene tested presented neither significant nor tendentious elevation in gene expression (Fig. 10).

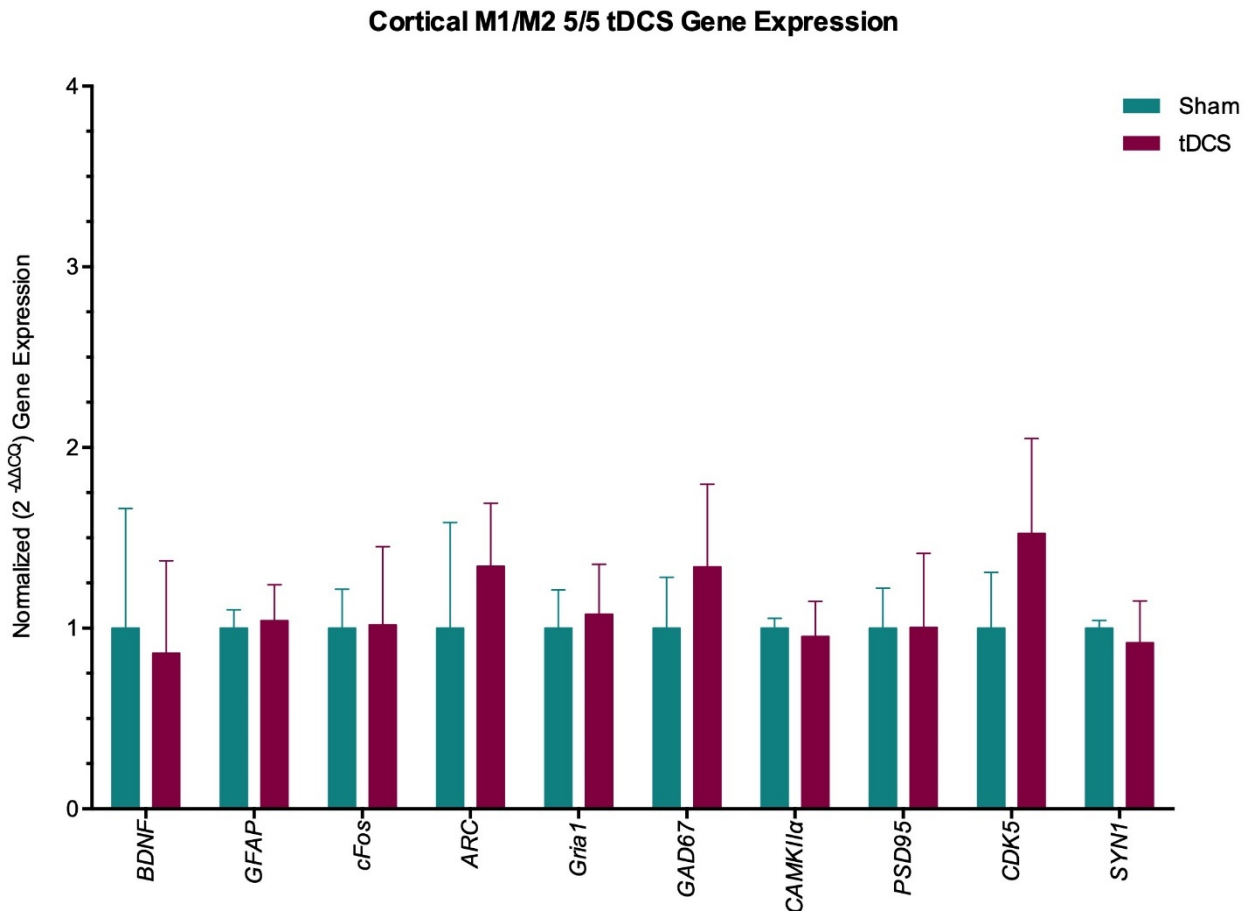


**Figure 10. Gene expression changes evoked by tDCS in group 5/5.**

Quantitative polymerase chain reaction gene expression. tDCS (Magenta/ $n=4$ ) vs. Sham (Green/ $n=4$ ). Stimulated group received currents 10 minutes of 350  $\mu$ A for 5 days (1 sessions/day). Tissue for gene expression collected 5 days after last stimulation. Data for mRNA levels shows *BDNF* ( $p = 0.5824$ ), *GFAP* ( $p = 0.7839$ ), *cFos* ( $p = 0.9731$ ), *ARC* ( $p = 0.8867$ ), *Gria1* ( $p = 0.8248$ ), *GAD67* ( $p = 0.3825$ ), *CAMKII $\alpha$*  ( $p = 0.8556$ ), *PSD95* ( $p = 0.9240$ ), *CDK5* ( $p = 0.1881$ ) and *SYN1* ( $p = 0.7893$ ) (from left to right). Groups were tested for normality under the D'Agostino-Pearson test followed by unpaired parametric Student's t-test to determine differences between means. Gene expression changes were calculated using the  $2^{-\Delta\Delta CQ}$  method relative to *RPL13A* gene. Data are expressed as mean and  $\pm$  S.E.M. error bars.

Furthermore, chronicity dependence was tested with the 10/1 group. The supposition was of that more sessions of tDCS would evoke even higher levels of gene expression and possibly present a differential expression profile. Among the same genes tested for groups 5/1 and 5/5 no significant differences were detected in group 10/1 (Fig. 11).

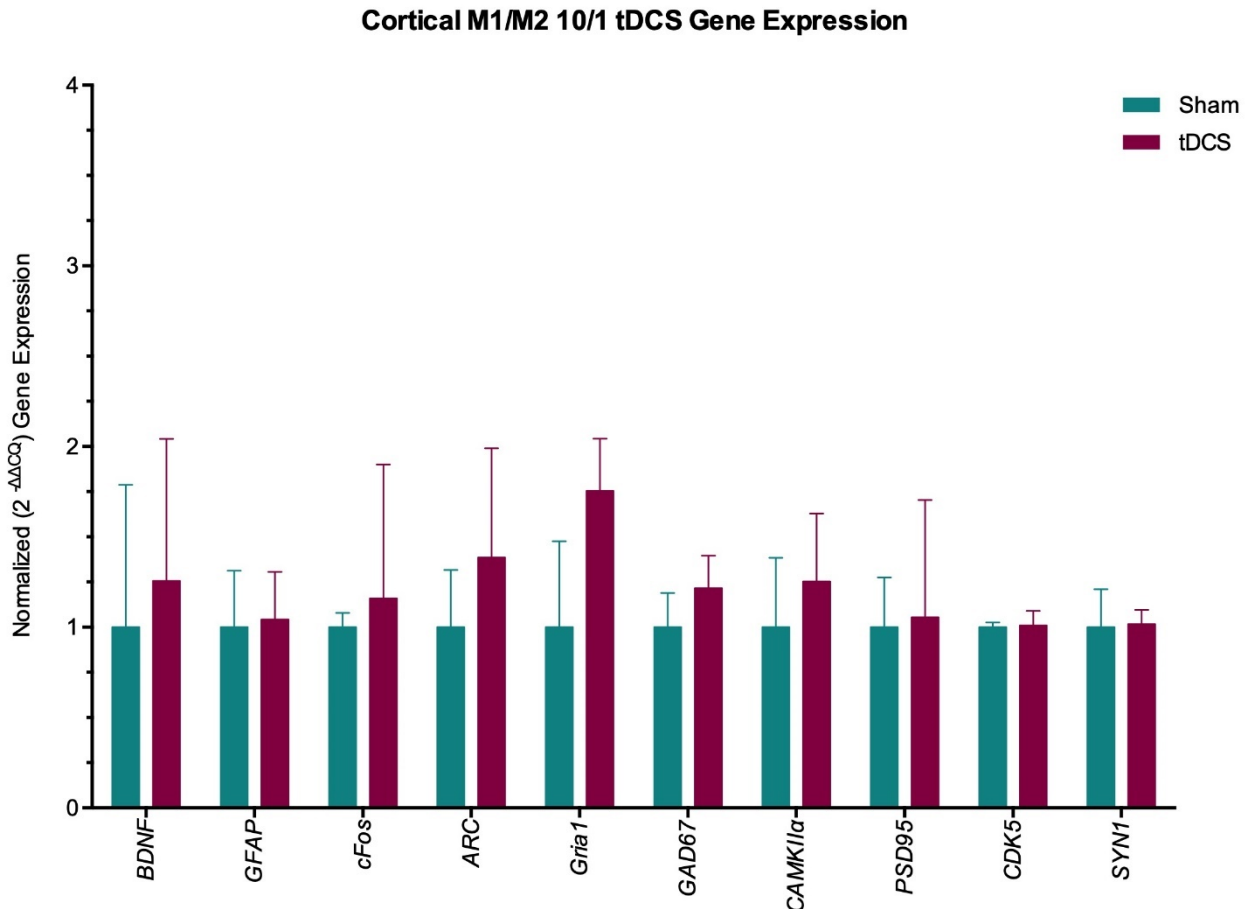


**Figure 11. Gene expression changes evoked by tDCS in group 10/1.**

Quantitative polymerase chain reaction gene expression. tDCS (Magenta/ $n=4$ ) vs. Sham (Green/ $n=4$ ). Stimulated group received currents 10 minutes of 350  $\mu$ A for 10 days (1 sessions/day). Tissue for gene expression collected 1 day after last stimulation. Data for mRNA levels shows *BDNF* ( $p = 0.4216$ ) *GFAP* ( $p = 0.9020$ ), *cFos* ( $p = 0.6923$ ), *ARC* ( $p = 0.3938$ ), *Gria1* ( $p = 0.1023$ ), *GAD67* ( $p = 0.1942$ ), *CAMKIIα* ( $p = 0.5924$ ), *PSD95* ( $p = 0.8451$ ), *CDK5* ( $p = 0.8369$ ) and *SYN1* ( $p = 0.9830$ ) (from left to right). Groups were tested for normality under the D'Agostino-Pearson test followed by unpaired parametric Student's t-test to determine differences between means. Gene expression changes were calculated using the  $2^{-\Delta\Delta CQ}$  method relative to *RPL13A* gene. Data are expressed as mean and  $\pm$  S.E.M. error bars.

## 5.2.0 tDCS task-paired group behavioral and genetic profile.

In addition to analyzing expression alterations a behavioral model was developed to test whether anodal tDCS could improve learning task performance (see materials and methods for behavioral assessment and task-paired procedures and groups for further understanding).

Memory enhancement via tDCS has already been shown in the body of literature, since it is a common presented feature in tDCS performance in both mice and humans, the Barnes Maze (an untested maze for tDCS performance) was used to further explore our animal mode. Basal behavioral performance was assessed through an initial task habituation protocol testing whether both groups (non-stimulated) presented similar performance. For this me analyzed total distance travelled, total errors and total mean speed. As seen in figure 12 no statistical differences were detected between both groups (Fig. 12).

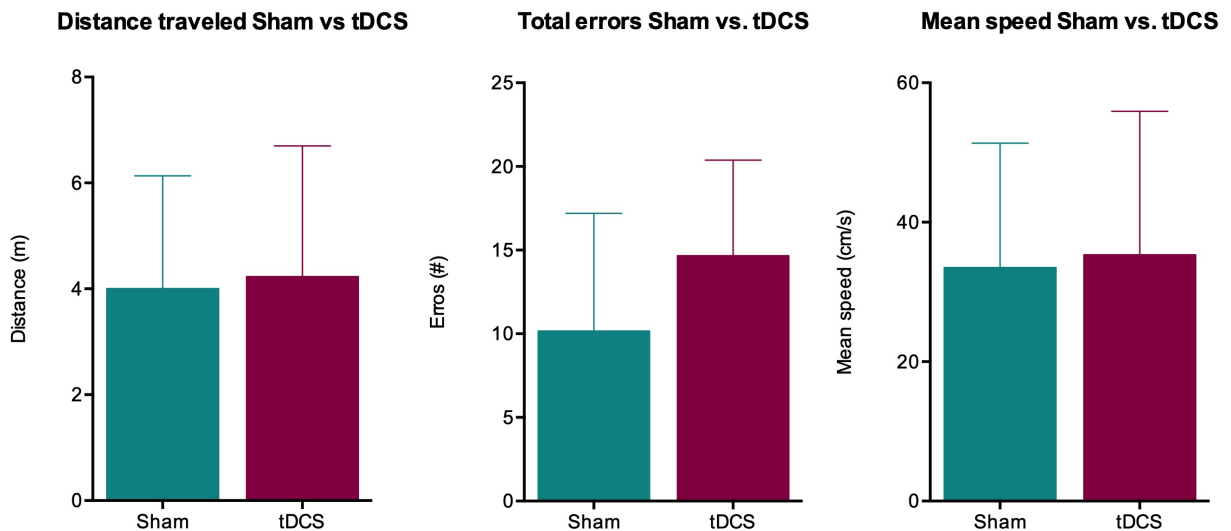


**Figure 12. Task-paired habituation performance.**

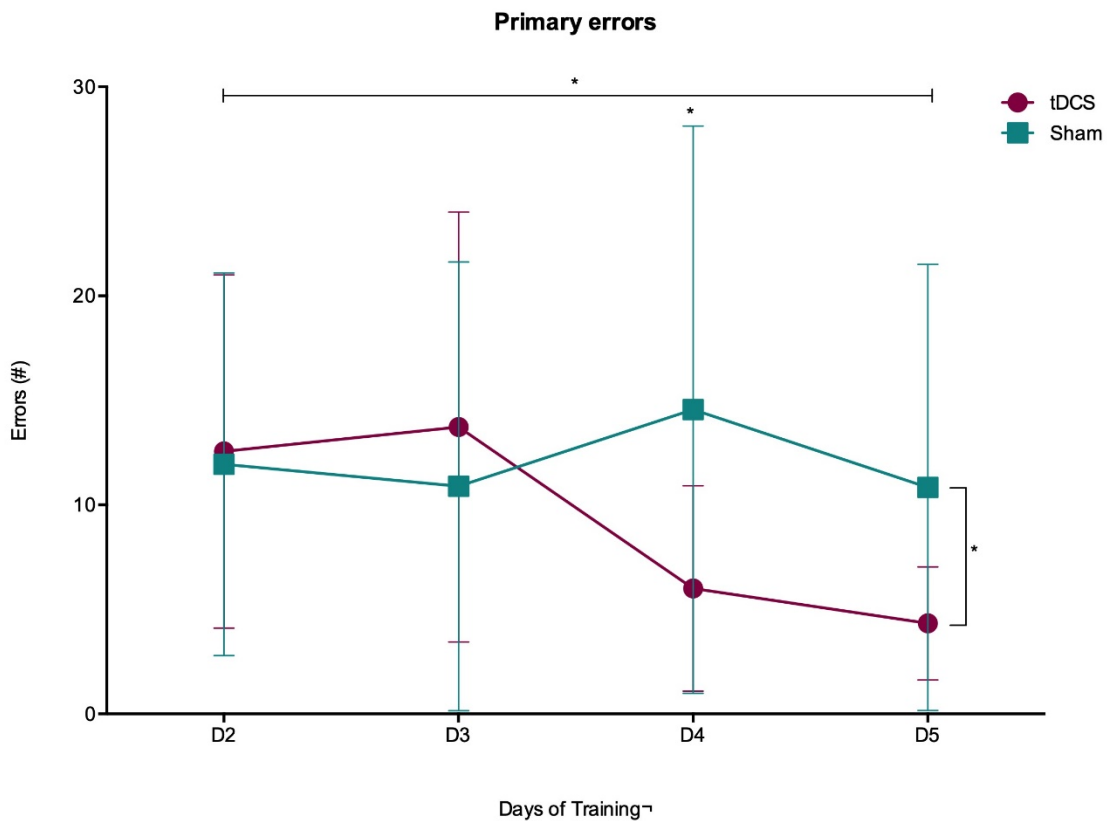
Task-paired habituation performance non-stimulated tDCS vs. tDCS (Magenta/ $n=6$ ) vs. Sham (Green/ $n=6$ ) Sham showing to the left, total Distance Traveled ( $p = 0.9999$ ), in the middle, total Errors ( $p = 0.2922$ ) and on the right, total Mean speed ( $p = 0.9999$ ) Groups were tested for normality under the D'Agostino-Pearson test followed by unpaired nonparametric Mann-Whitney U-test to determine differences between means. Data are expressed as mean and  $\pm$  S.E.M. error bars.



In the habituation period due to it being the first exposure of the animals to the apparatus primary data and total latency were not analyzed since these are dependent on the animal finding the escape hole.

Habituation was followed by a 4-day task training to quantify learning curves. During task days tDCS group animals received 350  $\mu$ A of electric current for 10 minutes 20 minutes after the last of three daily trials. Here we tested primary and total performance on all the parameters cited in the materials and methods for behavioral assessment.

We initially tested whether the stimulated group animals would commit less primary and total errors during the 4-day task compared to the non-stimulated sham group. Figure 13 shows general progression in performance (fewer errors being committed) from day 2 to 5 (day 1 is habituation) in primary errors (top image) and total errors (bottom image). tDCS group presented statistically less errors compared to sham group in general, with a standing out performance in day 4 for primary errors and in day 5 for total errors (Fig. 13).



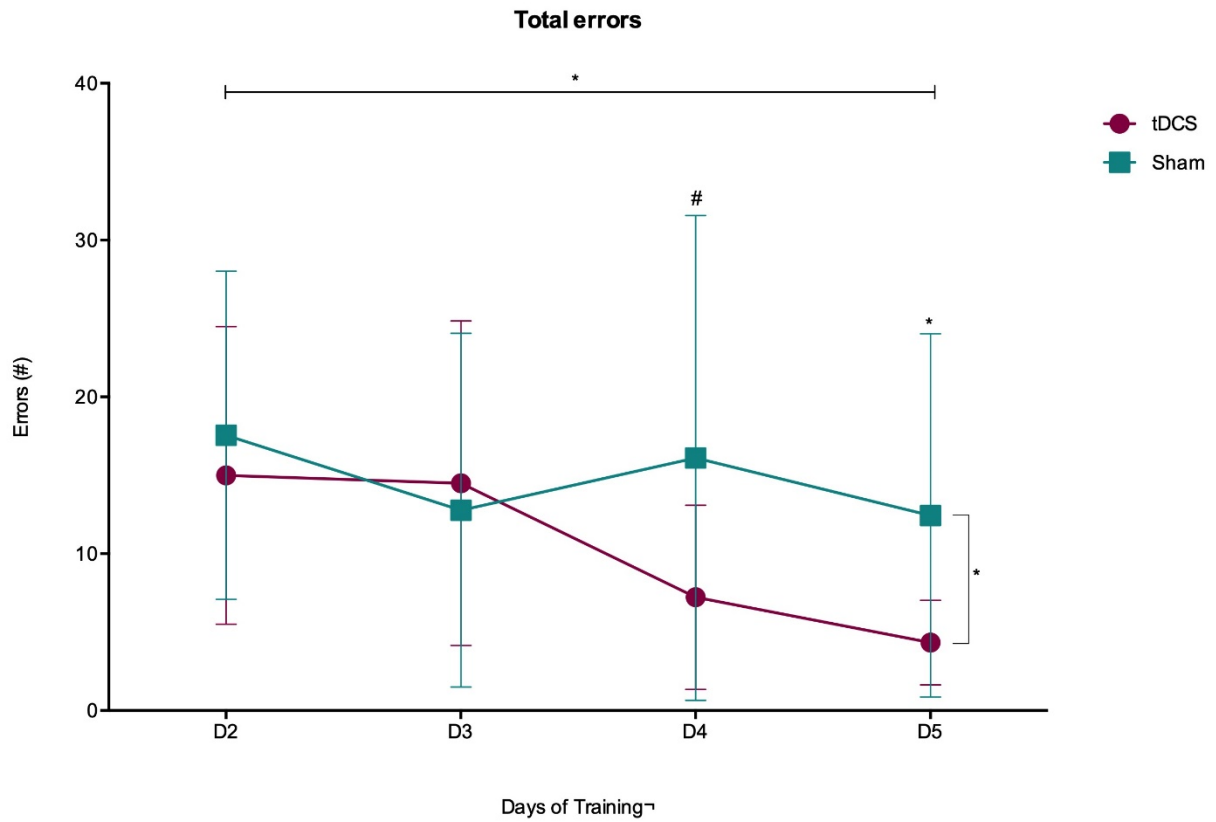


**Figure 13. Task-paired primary and total errors.**

Task-paired training performance of 4 days, from day 2 (D2) to day 5 (D5). (Magenta/ $n=6$ ) vs. Sham (Green/ $n=6$ ). Sham Top image shows primary errors. General day 2 to day 5 progression (day factor, top bar –  $p = 0.0396$ ) and mean difference in treatment performance for tDCS (treatment, side bar –  $p = 0.0463$ ) specifically in day 4 (D4 –  $p = 0.0281$ ). Bottom image shows total errors. General day 2 to day 5 progression (day factor, top bar –  $p = 0.0118$ ) and mean difference in treatment performance for tDCS (treatment, side bar –  $p = 0.0173$ ) specifically in day 5 (D5 –  $p = 0.0421$ ) and a tendency in day 4 (D4 –  $p = 0.0761$ ). Groups were tested by day using the D'Agostino-Pearson normality followed by Two-wat ANOVA (Sidak's). Data are expressed as mean and  $\pm$  S.E.M. error bars. *n.s.* = nonsignificant, # = strong tendency ( $p \leq 0.05 - \geq 0.10$ ),  $p \leq 0.05^*$ ,  $p \leq 0.01^{**}$ .

Furtherly, we tested if animals under stimulation took less time to perform the task (locate the escape hole) compared to the non-stimulated animals. Figure 14 shows general progression in performance (less time to find the escape hole) from day 2 to 5 (day 1 is habituation) in primary latency (top image) and total latency (bottom image). tDCS group took statistically less time to perform the task compared to sham group in general, with a standing out performance in day 4 for primary latency and in day 5 for total latency (Fig. 14).

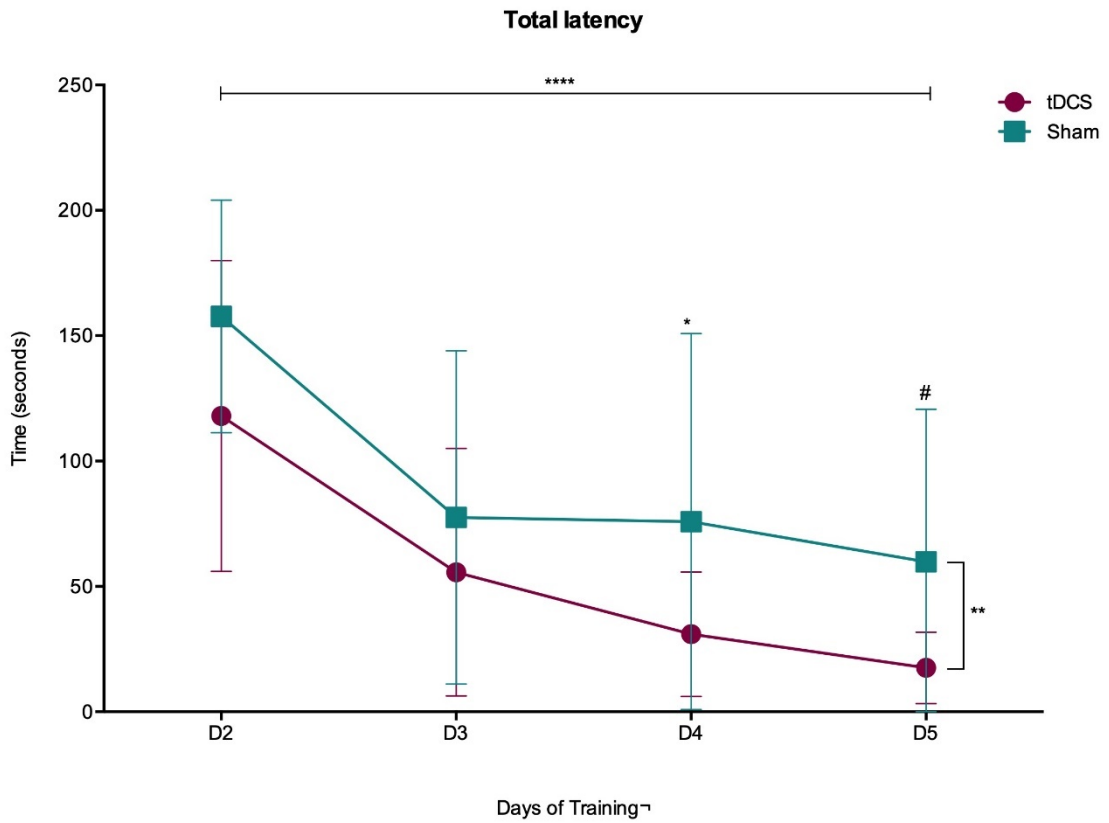
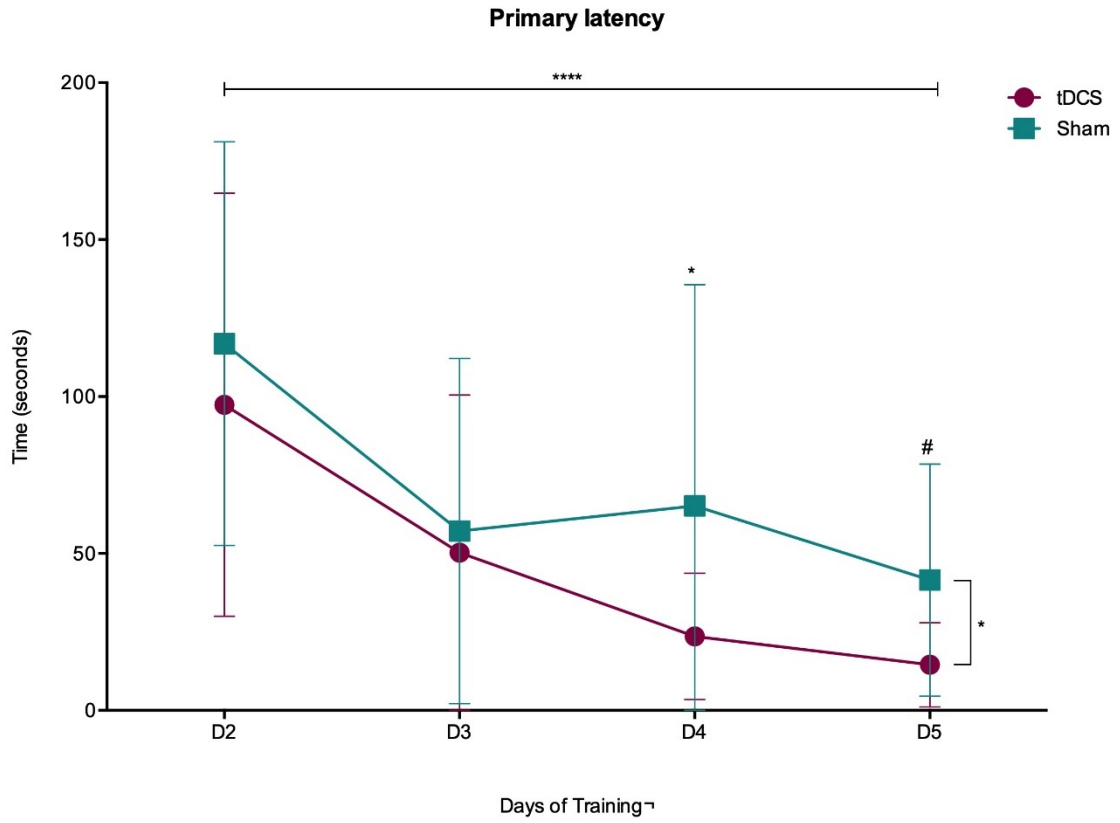


**Figure 14. Task-paired primary and total latency.**

Task-paired training performance of 4 days, from day 2 (D2) to day 5 (D5). (Magenta/ $n=6$ ) vs. Sham (Green/ $n=6$ ). Top image shows primary latency. General day 2 to day 5 progression (day factor, top bar –  $p = 0.0001$ ) and mean difference in treatment performance for tDCS (treatment, side bar –  $p = 0.0409$ ) specifically in day 4 (D4 –  $p = 0.0478$ ) and a tendency in day 5 (D5 –  $p = 0.0673$ ). Bottom image shows total latency. General day 2 to day 5 progression (day factor, top bar –  $p = 0.0001$ ) and mean difference in treatment performance for tDCS (treatment, side bar –  $p = 0.0087$ ) specifically in day 4 (D4 –  $p = 0.0503$ ) and a tendency in day 5 (D5 –  $p = 0.0754$ ). Groups were tested by day using the D'Agostino-Pearson normality followed by Two-way ANOVA (Sidak's). Data are expressed as mean and  $\pm$  S.E.M. error bars. *n.s.* = nonsignificant, # = strong tendency ( $p \leq 0.05 - \geq 0.10$ ),  $p \leq 0.05^*$ ,  $p \leq 0.01^{**}$ ,  $p \leq 0.001^{***}$ ,  $0.0001^{****}$ .

In sequence, we tested if animals under stimulation traveled a smaller distance to complete the task compared to the non-stimulated animals. Figure 15 shows general progression in performance (smaller distance traveled to find the escape hole) from day 2 to 5 (day 1 is habituation) in primary distance (top image) and total distance (bottom image). tDCS group traveled a statistically smaller distance to perform the task compared to sham group in general, with a standing out performance in day 5 for primary and total distance (Fig. 15).

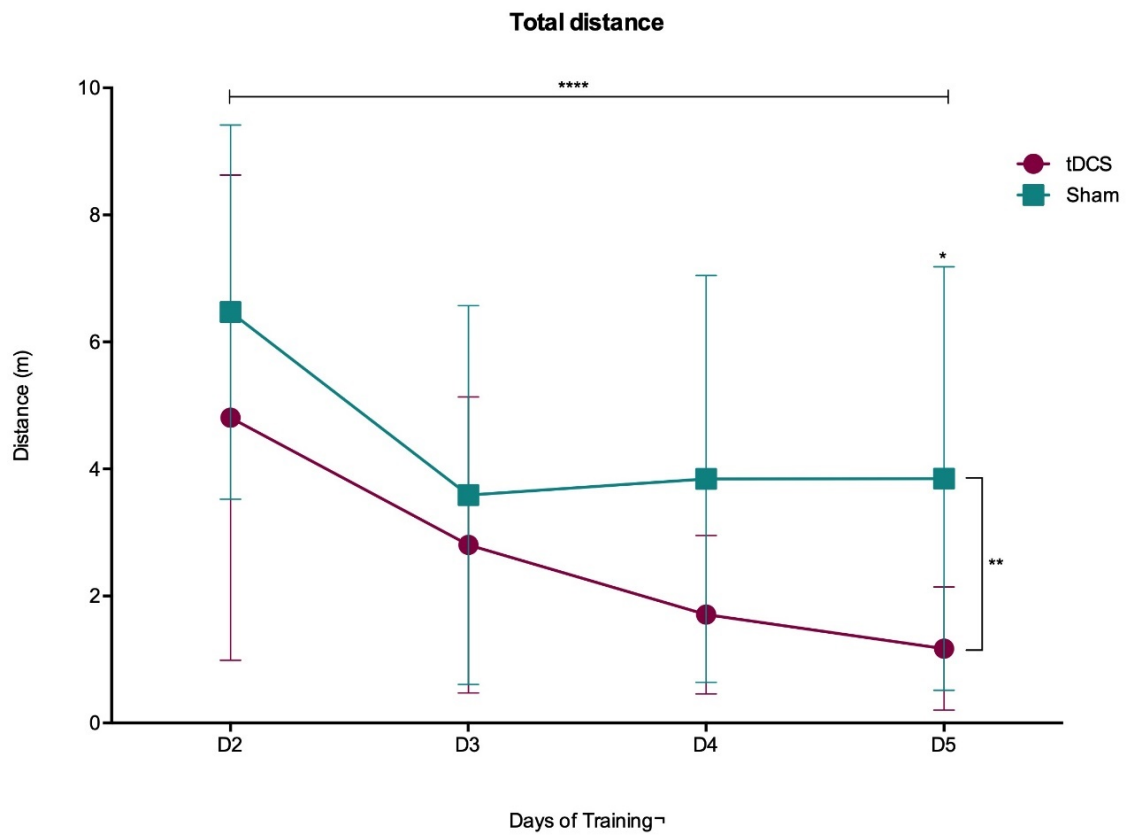
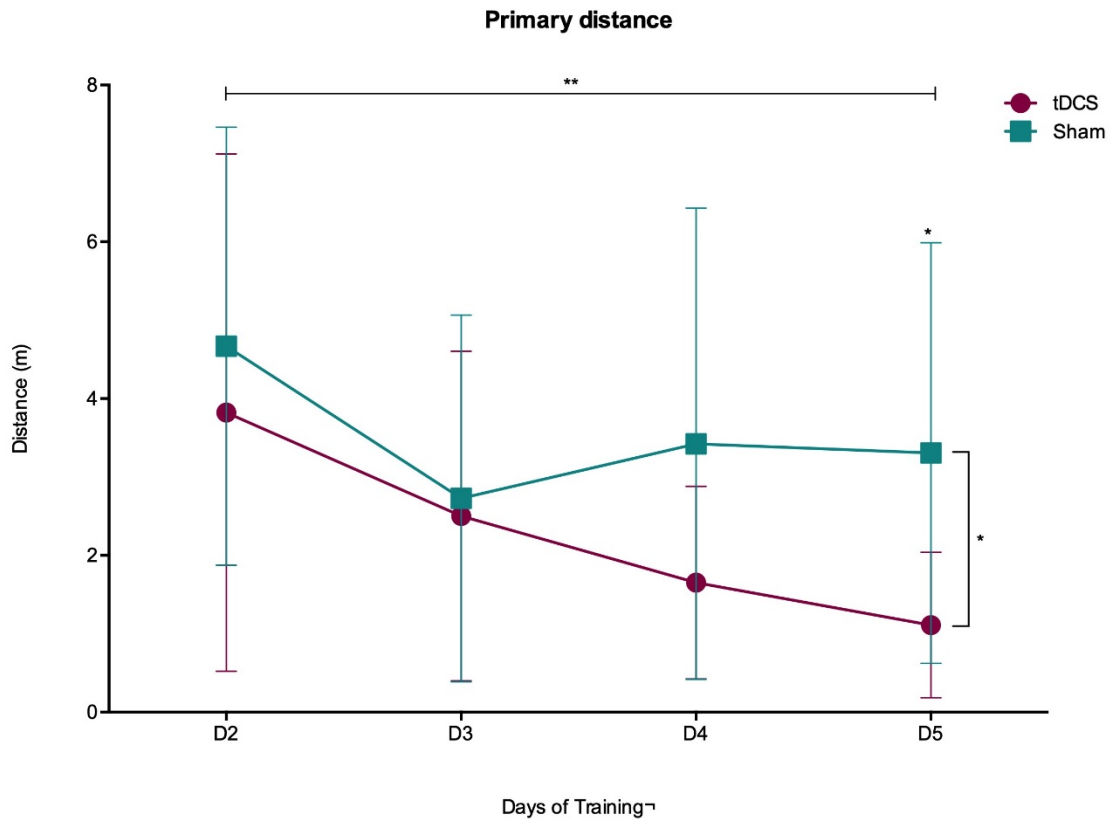


**Figure 15. Task-paired primary and total distance traveled.**

Task-paired training performance of 4 days, from day 2 (D2) to day 5 (D5). tDCS (Magenta lines and circles/ $n=6$ ) vs. Sham (Green lines and squares/ $n=6$ ). Top image shows primary distance. General day 2 to day 5 progression (day factor, top bar –  $p = 0.0012$ ) and mean difference in treatment performance for tDCS (treatment, side bar –  $p = 0.0105$ ) specifically in day 5 (D5 –  $p = 0.00298$ ). Bottom image shows total distance. General day 2 to day 5 progression (day factor, top bar –  $p = 0.0001$ ) and mean difference in treatment performance for tDCS (treatment, side bar –  $p = 0.0037$ ) specifically in day 5 (D5 –  $p = 0.0098$ ). Groups were tested by day using the D'Agostino-Pearson normality followed by Two-wat ANOVA (Sidak's). Data are expressed as mean and  $\pm$  S.E.M. error bars. *n.s.* = nonsignificant, # = strong tendency ( $p \leq 0.05 - \geq 0.10$ ),  $p \leq 0.05^*$ ,  $p \leq 0.01^{**}$ ,  $p \leq 0.001^{***}$ ,  $0.0001^{****}$ .

Due to an increased performance of the stimulated group in primary and total errors, latency and distance traveled, and considering the stimulated area being fundamental for motor execution (M1 and M2) mean speed from day 2 to day 5 was analyzed (day 1 is habituation) to eliminate the possibility of motor enhancement. Figure 16 shows no statistical difference in mean speed performance between the tDCS and Sham group (Fig. 16).

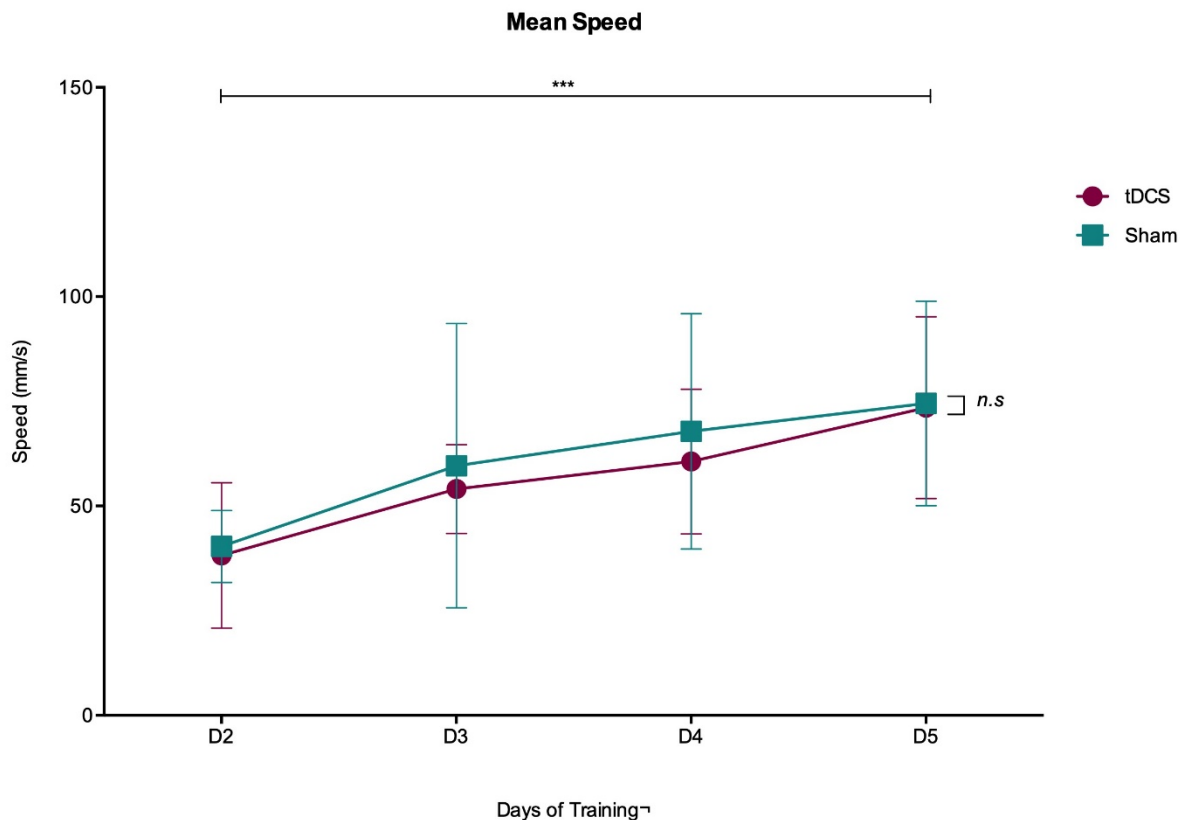


**Figure 16. Task-paired mean speed performance.**

Task-paired training performance of 4 days, from day 2 (D2) to day 5 (D5). tDCS (Magenta lines and circles/ $n=6$ ) vs. Sham (Green lines and squares/ $n=6$ ). Image shows mean speed performance. General day 2 to day 5 progression (day factor, top bar –  $p = 0.0011$ ) and mean difference in treatment performance for tDCS (treatment, side bar –  $p = 0.8906$ ). Groups were tested by day using the D'Agostino-Pearson normality followed by Two-wat ANOVA (Sidak's). Data are expressed as mean and  $\pm$  S.E.M. error bars. *n.s.* = nonsignificant, # = strong tendency ( $p \leq 0.05 - \geq 0.10$ ),  $p \leq 0.05^*$ ,  $p \leq 0.01^{**}$ ,  $p \leq 0.001^{***}$ ,  $0.0001^{****}$ .

Furthermore, in the attempt of understand enhanced performance we looked at general search strategies. Figure 17 shows how all animals (tDCS+Sham) responded to the daily trainings in terms of used strategies and saw that with the pass of days animals tended to use less of the random strategies and more direct and serial ones (Fig. 17).

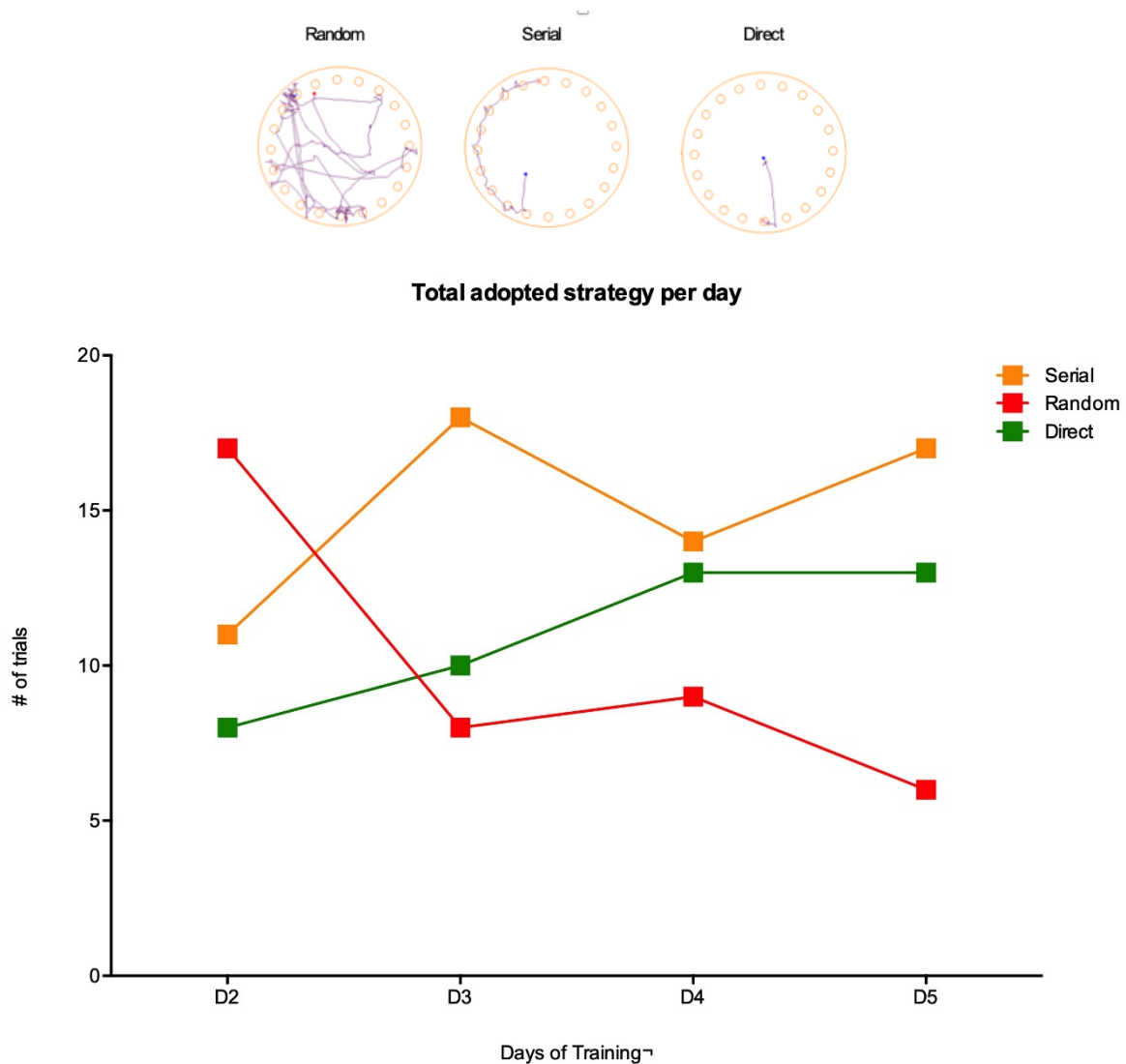


**Figure 17. Task-paired general use of strategies.**

Top figure shows a tracer chart of 3 distinct animals using, from left to right, direct, serial and random strategies. Bottom figure shows task-paired training use of strategies from day 2 to day 5 (tDCS+Sham). Red squares and lines illustrate the use of random strategies, yellow squares and lines represent serial strategies and green squares and lines the use of direct strategies.

After confirming differential use of strategies among days we furthered asked if strategies reflected enhanced performance. This was done by analyzing strategy efficiency considering to primary errors, primary latency and primary distance. Figure 18 shows that a significant less amount of errors are committed as well as less time spent, and smaller distance traveled when adopting direct and serial strategies compared to the random one (Fig. 18).

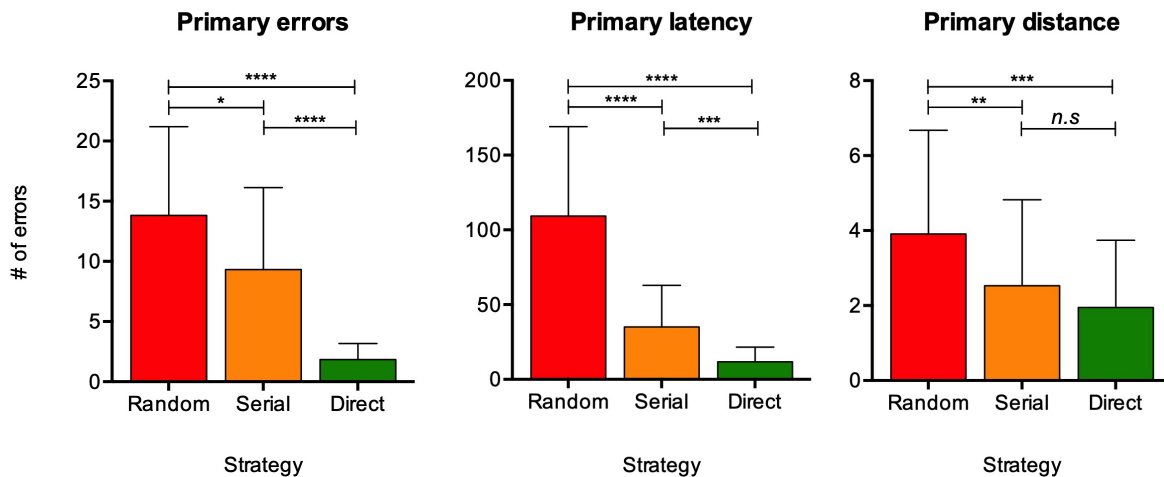


**Figure 18. Task-paired general use of strategies.**

Task-paired strategy performance of general groups (tDCS+Sham). Figure to the left comparing strategies (red bar = random, orange bar = serial and green bar = direct), random vs. direct (top bar –  $p = 0.0001$ ) random vs. serial (middle bar –  $p = 0.0182$ ) and serial vs. direct (bottom bar –  $p = 0.0001$ ) in function of primary errors. Middle figure shows random vs. direct (top bar –  $p = 0.0001$ ) random vs. serial (middle bar –  $p = 0.0001$ ) and serial vs. direct (bottom bar –  $p = 0.0023$ ) in function of primary latency and right figure shows random vs. direct (top bar –  $p = 0.0002$ ) random vs. serial (middle bar –  $p = 0.0057$ ) and serial vs. direct (bottom bar –  $p = 0.8083$ ) in function of distance. Groups were tested under ANOVA (Kruskal-Wallis test) for multiple comparisons. Data are expressed as mean and  $\pm$  S.D. error bars. *n.s.* = nonsignificant, # = strong tendency ( $p \leq 0.05 - \geq 0.10$ ),  $p \leq 0.05^*$ ,  $p \leq 0.01^{**}$ ,  $p \leq 0.001^{***}$ ,  $0.0001^{****}$ .



To conclude, we analyzed the total use of strategies per group (Sham vs. tDCS). Figure 19 shows a comparison of the tDCS vs. Sham of total adopted strategies (sum of days) for direct, serial and random (Fig. 19).

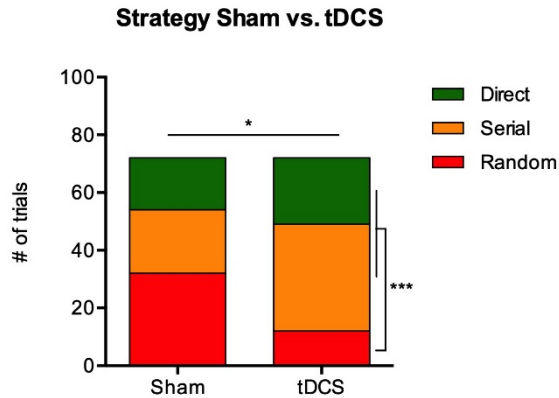


**Figure 19. Strategy use of tDCS vs. Sham.**

Total use strategies comparing tDCS vs. Sham. Types of strategies direct (green), serial (orange) and random (red) strategies of comparison of differences between groups (top bar –  $p = 0.0356$ ), differences in tDCS group (Direct+Serial vs. Random) (side bar –  $p = 0.0003$ ) and differences in sham group (Direct+Serial vs. Random) (not shown –  $p = 0.1121$ ). Groups were tested under the Chi-square test. Data are expressed as mean and  $\pm$  S.D. error bars. *n.s.* = nonsignificant, # = strong tendency ( $p \leq 0.05 - \geq 0.10$ ),  $p \leq 0.05^*$ ,  $p \leq 0.01^{**}$ ,  $p \leq 0.001^{***}$ ,  $0.0001^{****}$ .

A genetic profile was also investigated for animals that underwent the task-paired stimulation under the assumption that equal or stronger modulation would be evoked since the stimulation protocol was similar to the 5/1 with the additional evoked modulation of a complex learning task. Figure 20 shows a significant decrease in the *cFos* gene (neuronal activity marker) expression which was not found in any other group and a mild tendency in BDNF expression. In addition, no other gene presented alterations in expression.

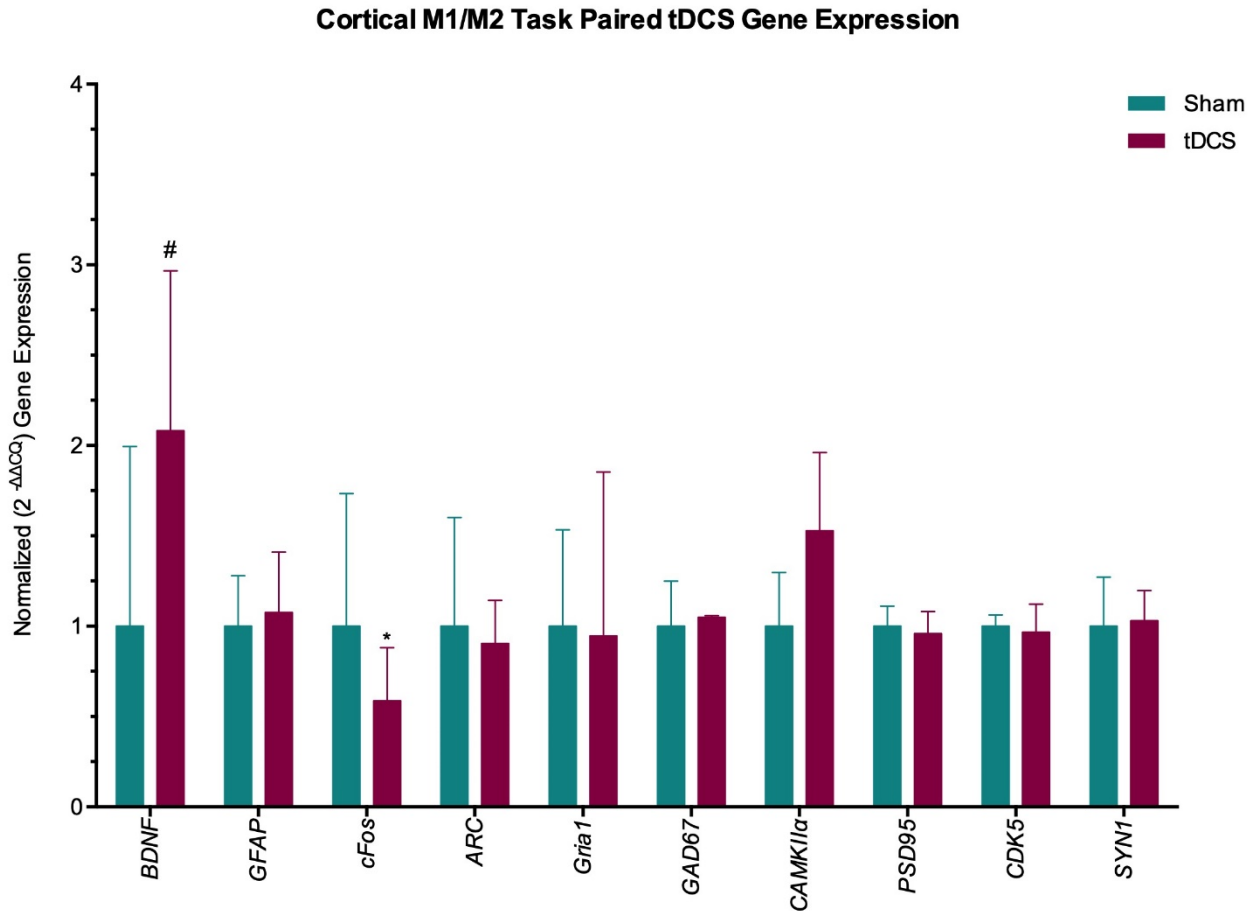


**Figure 20. Gene expression changes evoked by tDCS in group task-paired.**

Quantitative polymerase chain reaction gene expression. tDCS (Magenta bar/ $n=4$ ) vs. Sham (Green bar/ $n=4$ ). Stimulated group received currents 10 minutes of 350  $\mu$ A for 10 days (1 sessions/day). Each stimulation session was carried out 20 minutes after the last daily trial of the task. Tissue for gene expression collected 1 day after last stimulation. Data for mRNA levels shows *BDNF* ( $p = 0.0607$ ), *GFAP* ( $p = 0.6350$ ), *cFos* ( $p = 0.0370$ ), *ARC* ( $p = 0.2409$ ), *Gria1* ( $p = 0.5587$ ), *GAD67* ( $p = 0.5292$ ), *CAMKII $\alpha$*  ( $p = 0.1535$ ), *PSD95* ( $p = 0.3464$ ), *CDK5* ( $p = 0.8369$ ) and *SYN1* ( $p = 0.9830$ ) (from left to right). Groups were tested for normality under the D'Agostino-Pearson test followed by unpaired parametric Student's t-test to determine differences between means. Gene expression changes were calculated using the  $2^{-\Delta\Delta C_t}$  method relative to *RPL13A* gene. Data are expressed as mean and  $\pm$  S.E.M. error bars.

## 5.2.0 Cortical assessment of total glutamate determination.

Additionally, with the attempt to show increased neuronal activity tDCS stimulated mice we prepared tissue for cortical M1 and M2 total glutamate determination. Analysis in

figure shows that, although the task-paired group presented higher levels of glutamate concentration in general no significant amount was detected between stimulated and non-stimulated animals (Fig. 21).

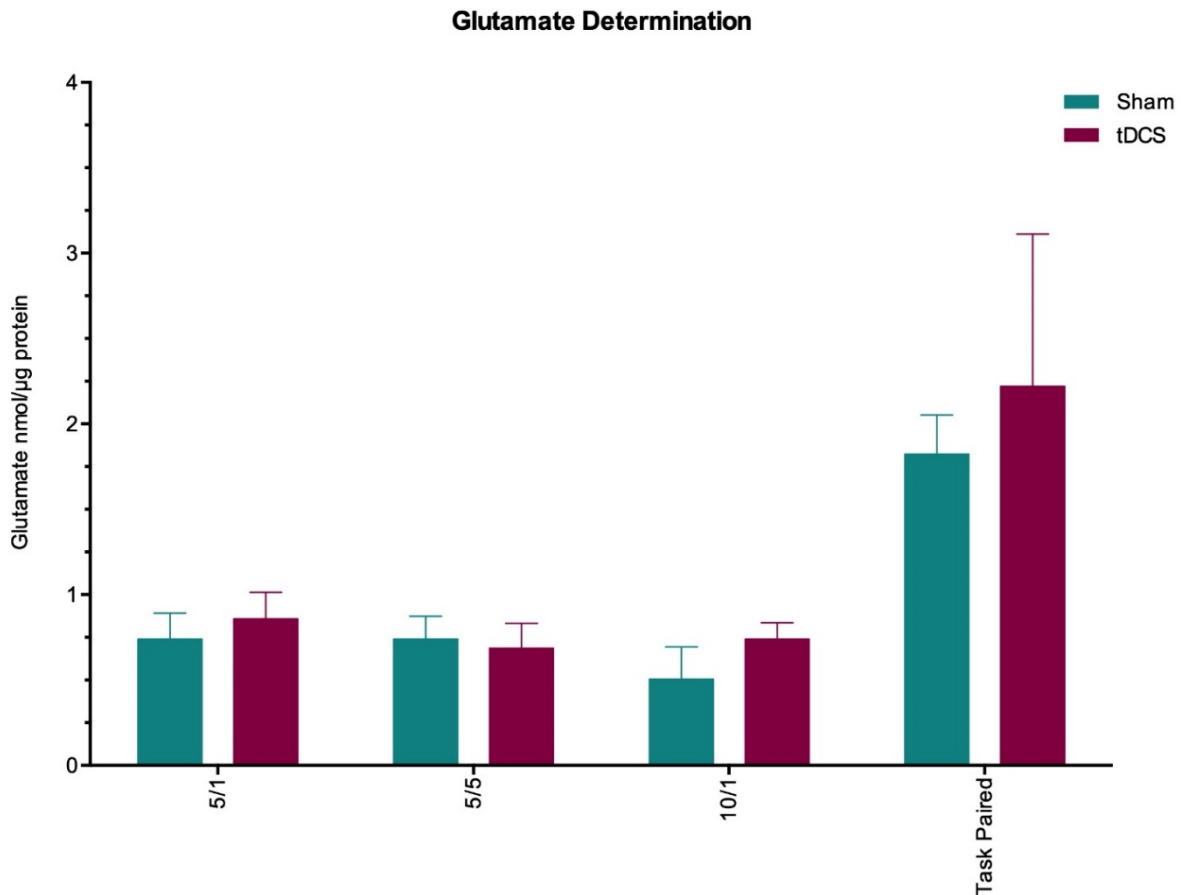
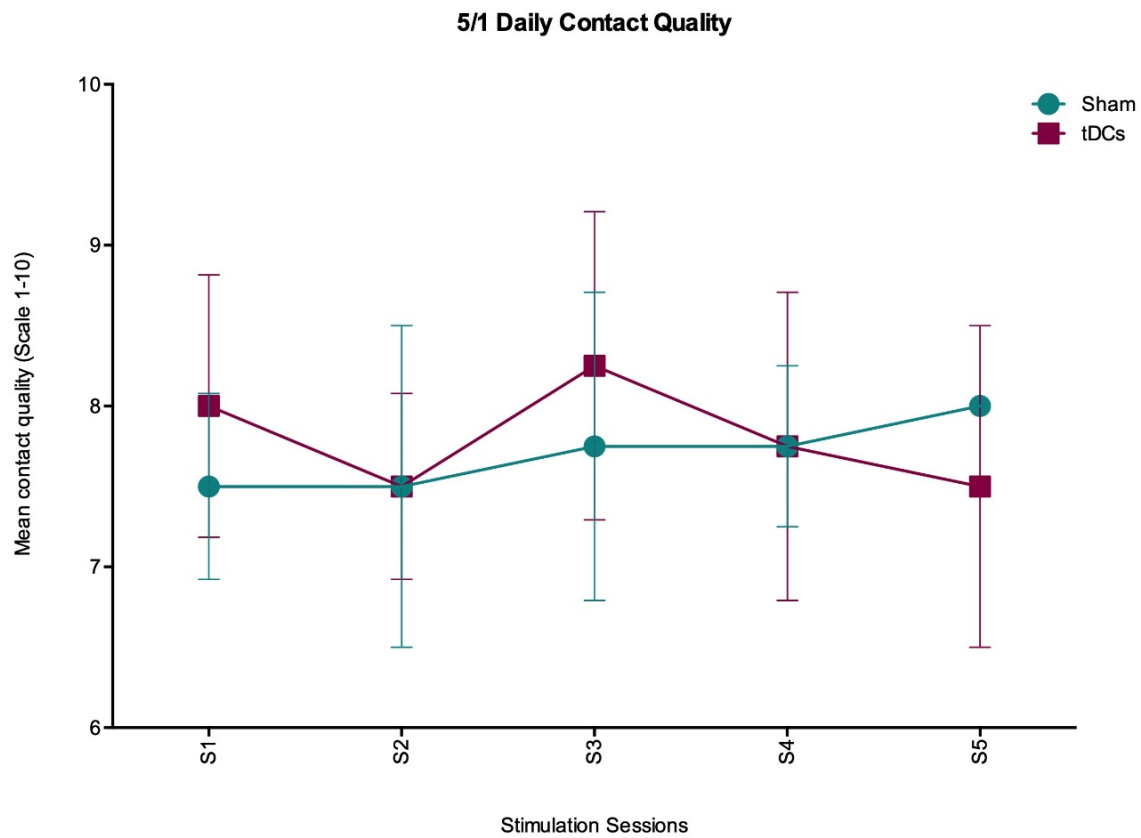


**Figure 21. Total cortical glutamate determination.**

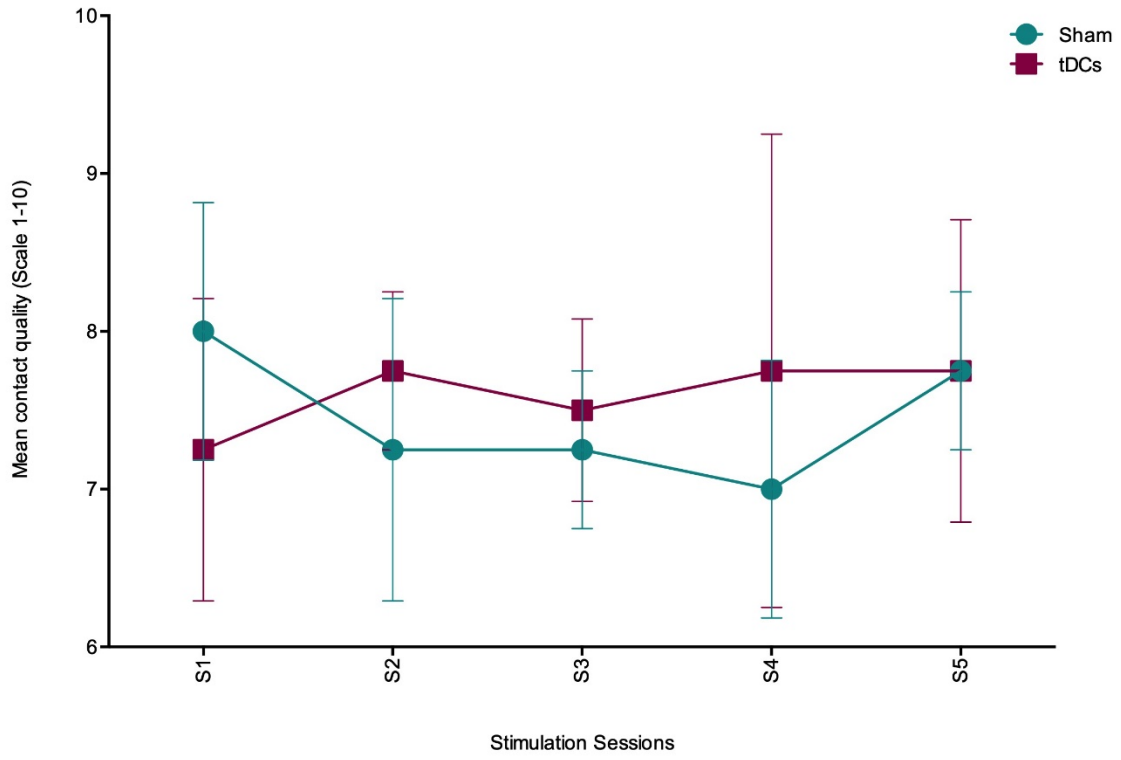
Assessment of cortical glutamate for groups 5/1, 5/5, 10/1 and task-paired (from left to right). tDCS (Magenta/ $n=6$ ) vs. Sham (Green/ $n=6$ ). No significant difference was detected in glutamate concentration in group 5/1 ( $p = 0.3130$ ), 5/5 ( $p = 0.6249$ ), 10/1 ( $p = 0.1002$ ) and 0.3160. Groups were tested for normality under the D'Agostino-Pearson test followed by unpaired nonparametric Mann-Whitney U-test to determine differences between means. Data are expressed as mean and  $\pm$  S.E.M. error bars.

### 5.3.0 tDCS implant and electrode viability.

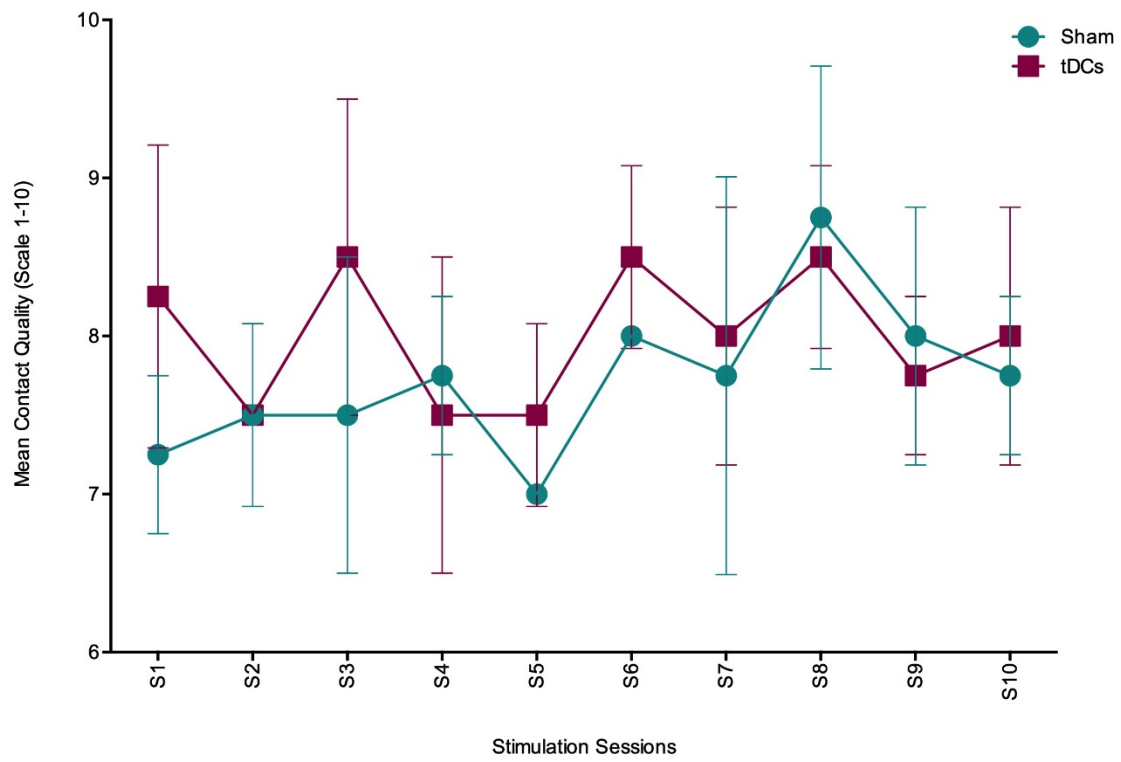
To overlap any implant and electrode stability or viability, we further registered the contact quality of each stimulation session for each animal (mean/group) with the intention of identifying any unexpected complication. Figure shows contact quality of groups 5/1, 5/5, 10/1 and task-paired per day. No statistical differences were detected (Fig. 22).



### 5/5 Contact Quality



### 10/1 Contact Quality



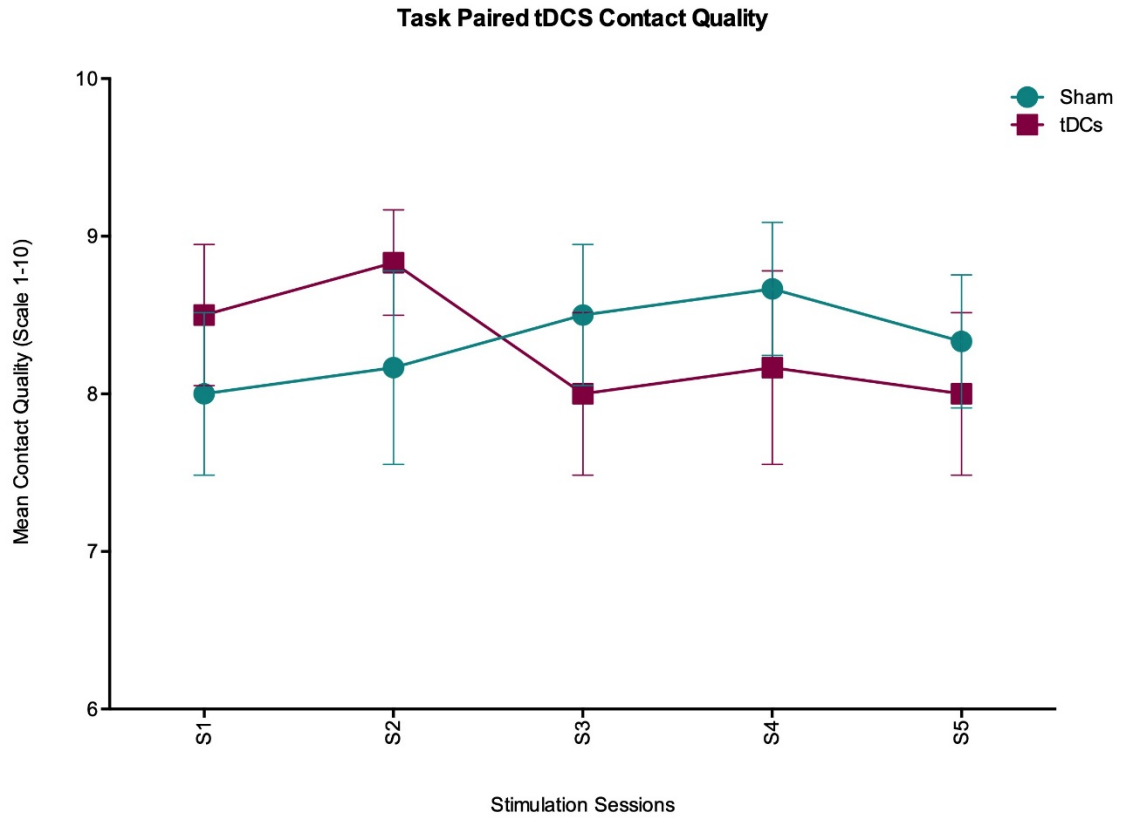


**Figure 22. Contact quality for groups 5/1, 5/5, 10/1 and task-paired.**

Contact quality from anode to cathode circuit of groups 5/1, 5/5, 10/1 and task-paired. (tDCS+Sham). From top to bottom, 5/1 contact quality general progression (day factor –  $p = 0.8109$ ), and mean difference in treatment contact quality for tDCS (treatment –  $p = 0.6940$ ), 5/5 contact quality general progression (day factor –  $p = 0.4803$ ), and mean difference in treatment contact quality for tDCS (treatment –  $p = 0.5859$ ), 10/1 contact quality general progression (day factor –  $p = 0.1935$ ), and mean difference in treatment contact quality for tDCS (treatment –  $p = 0.1038$ ) and task-paired contact quality general progression (day factor –  $p = 0.6515$ , and mean difference in treatment contact quality for tDCS (treatment –  $p = 0.8315$ ). Data are expressed as mean and  $\pm$  S.E.M. error bars.

## **6.0 DISCUSSION**

A discussion on the surgical and stimulation model validation may be found in the article above, therefore will not be cited here.

### **6.1.0 tDCS induces gene expression alterations.**

tDCS was able to effectively evoke gene expression alterations in a protocol dependent manner. Specifically, by stimulating mice for 5 days, one session per day at a current of 350  $\mu$ A for 10 minutes over the M1 and M2 cortical areas, tDCS was able to increase gene expression around *BDNF* and *GFAP*.

*BDNF* has been seen to present survival and growth promoting properties in several types of neurons, especially in the hippocampal and cortical areas (BEKKERS *et al.*, 2011). Partially knocked-out mice for *BDNF* (+/-) have previously presented impaired spatial learning and cognitive decline, a common mark for neuropsychiatric diseases (BARTOLLETTI *et al.*, 2002).

*GFAP* is a well-known hallmark for astrocytes. It is responsible for composing astrocyte communication filaments and increase astrocyte-neuron and neuron-neuron communication. Astrocytes play an important role in mediating synaptic activity and are also viewed as important metabolic pathways between blood vessels and other neuronal cells. Interestingly a higher count, and, increased astrocyte activation has also been correlated to improved cognitive functions.

Furthermore, both genes have already been strongly correlated to tDCS mechanisms. Studies corroborated that by inhibiting *BDNF* or blocking astrocyte activity, all behavioral and plasticity alterations evoked by tDCS are seized (PODDA *et al.* 2016 and MONAI *et al.*, 2016). Therefore, the results presented here do not surprise the body of literature. In contrast, as increased expressions were only found in the 5/1 group a wider discussion on protocol stimulation and *BDNF/GFAP* expression present itself as a data yet to be seen by the scientific community.

Initially, by repeating stimulation sessions to 5/1 but allowing mice to rest for an additional 4 days (5/5) before collecting neuronal tissue, we identified that the gene expression evoked in 5 sessions of stimulation are not persistent. This data is important once astrocyte activation and *BDNF* levels have already been associated to increased



cognitive and physical activity. Therefore, current stimulation protocols with long period durations between each battery of sessions may be flawed and that by shortening this period, tDCS' effects may be potentiated and persist for longer durations.

In addition, by increasing stimulation from a 5-day (1 session/day) stimulation to a 10-day (1 session/day) stimulation expression was also extinguished. This data may suggest a negative feedback mechanism around gene expression activity. Due to increased stimulation activity, there may have been a saturation in gene expression, causing neurons to both lower cellular activity and negatively modulating gene expression. This result may sustain another flaw in stimulation protocols which are usually above 10 days of stimulation with one session per day.

In the task-paired group, although *GFAP* did not present altered expression, *BDNF* presented a strong tendency toward an increased expression, but with no statistical difference. This may have happened since performing tasks that have high cognitive demand, naturally evoke increased *BDNF* levels. Therefore, since both stimulated and non-stimulated groups were submitted to the task, cognitive-*BDNF* levels may have masked tDCS-*BDNF* increase.

Interestingly, among the selected genes in this project, tDCS seems to strictly evoke increased expression of these two genes. To further confirm assumptions of expression persistency and chronicity, additional studies should be carried out. The addition of a 1/1 (1 day of stimulation collecting tissue 24 hours later), 1/5 (one day of stimulation collecting tissue 5 days latter) and even other task-paired protocols models are necessary and will further allow us to see how these genes respond. Additional techniques, such as western-blotting, to verify protein concentration of these genes and immunofluorescence, to investigate protein location in specific cell populations could also fortify further assumptions.

### **6.2.0 tDCS induces learning enhancement.**

In accordance to several other experimental articles, the enhancement in learning mediated by tDC stimulation has already been described. Podda *et al.*, (2016) demonstrated through a 1-stimulation session (350  $\mu$ A for 20 minutes) in mice, how *BDNF*

expression surges are acetylation dependent and mediate enhanced learning process using the Morris Water Maze task (a very similar task to the Barnes Maze, although a bit more aversive). In addition to exploring our model through gene alterations, we further developed a behavioral tDCS model focusing on learning acquisition. Our model presented, increased learning performance. Lowering in general number of errors committed, time taken, and distance travelled to execute the task. Non-stimulated mice also presented lower times and better performance towards the end of the experiments in days 4 and 5. However, seemingly, stimulated mice consistently and continuously presented a higher change in lowering numbers.

A crucial point was understanding how stimulated animals enhanced their performance. For this we investigated the adopted strategies. In general, we saw that animals that used more efficient strategies, such as the direct and serial ones, presented better performance compared to animals that used random ones. Over the task days, the stimulated mice seem to have adapted their choice over strategies and migrated to the most efficient ones. While non-stimulated mice also presented an alteration in strategy choice, there was no significant difference in preferences. The non-stimulated overall merged from higher random choices to a moderate increase in direct and serial ones. While stimulated animals significantly increase the number of direct and serial choices, lowering in general the use of random strategy.

### **6.3.0 tDCS does not affect total glutamate concentrations.**

There have been previously described results in which tDCS was shown to mediate higher glutamate surges through a *BDNF* pathway (MATTSON *et al.*, 2008). Studies have shown that tDCS' activity is primarily cortical and depending on electrode size and current intensity it may follow to subcortical regions through neuronal networks. Mostly, molecular investigations have been correlated to glutamate releasing neurons (pyramidal neurons) and astrocytes.

Since these have been shown as fundamental components for tDCS' efficiency and are directly correlated to glutamate surges we assumed that glutamate concentration would follow proportional *BDNF* expressions in each group. Even so, no significant

differences were detected in any of the groups. This result does not decouple tDCS *BDNF/Astrocyte*-glutamate association. Glutamate may respond by exclusively increasing its secretion mediated by LTP-like effects, but not increasing its synthesis.

To further investigate these assumptions, techniques such as synaptosome and brain microdialysis could allow the quantification of secretion rates.

#### **6.4.0 tDCS animal model implant viability and stability.**

Here many experiments have been executed with the proposed model. A common pointed out flaw in such experiments is that multiple and prolonged tDCS sessions may have a negative effect over the used implant and electrodes and may lead to false and dirty results. The over exposure of saline solution to the animal's cranium may cause the implant to become unstable. Furthermore, the increased number of stimulation sessions and heat generated may induce the formation of an inflammatory-like process hindering the stimulation efficiency. Through a daily registration of the contact quality between the target and reference anode we were able to demonstrate that in spite the alteration in protocols or context the implants and general stimulation sessions did not present any of these problems, maintaining the implants variable and tDCS efficient during all experiments.

## **7.0 OVERALL CONCLUSION AND FUTURE PERSPECTIVES**

- The proposed tDCS model presents a highly stable implant, with an easy and fast execution.
  - It proposes to increase tDCS animal studies in a simple manner and ease future investigations.
  - Its resulting gene expression alterations will work as a general marker of stimulation efficiency.
- Gene expression profile of the tDCS models depicts how important selecting protocols for stimulation is.
  - tDCS modulates gene expression in a restrict manner, here, exclusively for *BDNF* and *GFAP*.
  - Once directly related to cognition and skill performance *BDNF* and *GFAP* may both serve as markers to best select stimulation protocols.
- tDCS evoked behavioral alterations potentiating learning performance, showing an adaption in selected strategies looking towards a more efficient way to execute the task.
  - Further investigation in learning enhancement must be done with different tDCS protocols.
- tDCS does not increase total glutamate levels.
  - The results above do not abolish tDCS modulating glutamate.
  - Further investigations are necessary to test possible glutamate secretion facilitation via LTP.

## **REFERENCES**

1. Baker, J.M., Rorden, C., Fridriksson, J. Using transcranial direct-current stimulation to treat stroke patients with aphasia. *Stroke*. **41** (6), 1229–1236, doi: 10.1161/STROKEAHA.109.576785 (2010).
2. Bekkers, J.M. Pyramidal neurons. *Current Biology*. **21** (24), R975, doi: 10.1016/j.cub.2011.10.037 (2011).
3. Bennabi, D., Pedron, S., Haffen, E., Monnin, J., Peterschmitt, Y., Van Waes, V. Transcranial direct current stimulation for memory enhancement: from clinical research to animal models. *Frontiers in Systems Neuroscience*. **8**, 159, doi: 10.3389/fnsys.2014.00159 (2014).
4. Boggio, P.S. *et al.* Enhancement of non-dominant hand motor function by anodal transcranial direct current stimulation. *Neuroscience Letters*. **404** (1–2), 232–236, doi: 10.1016/j.neulet.2006.05.051 (2006).
5. Boggio, P.S. *et al.* Effects of transcranial direct current stimulation on working memory in patients with Parkinson's disease. *Journal of the Neurological Sciences*. **249** (1), 31–38, doi: 10.1016/J.JNS.2006.05.062 (2006).
6. Boggio, P.S. *et al.* Prolonged visual memory enhancement after direct current stimulation in Alzheimer's disease. *Brain Stimulation*. **5** (3), 223–230, doi: 10.1016/j.brs.2011.06.006 (2012).
7. Bramham, C.R., Messaoudi, E. BDNF function in adult synaptic plasticity: The synaptic consolidation hypothesis. *Progress in Neurobiology*. **76** (2), 99–125, doi: 10.1016/j.pneurobio.2005.06.003 (2005).
8. Brunoni, A.R. *et al.* Clinical research with transcranial direct current stimulation (tDCS): Challenges and future directions. *Brain Stimulation*. **5** (3), 175–195, doi: 10.1016/j.brs.2011.03.002 (2012).
9. Cosentino, G. *et al.* Anodal tDCS of the swallowing motor cortex for treatment of dysphagia in multiple sclerosis: a pilot open-label study. *Neurological Sciences*. **39** (8), 1471–1473, doi: 10.1007/s10072-018-3443-x (2018).
10. DaSilva, A.F., Volz, M.S., Bikson, M., Fregni, F. Electrode Positioning and Montage in Transcranial Direct Current Stimulation. *Journal of Visualized Experiments*. **5** (51), 42–46, doi: 10.3791/2744 (2011).
11. D'Mello, A.M., Turkeltaub, P.E., Stoodley, C.J. Cerebellar tDCS Modulates Neural Circuits during Semantic Prediction: A Combined tDCS-fMRI Study. *The Journal of Neuroscience*. **37** (6), 1604–1613, doi: 10.1523/JNEUROSCI.2818-16.2017 (2017).

12. Fregni, F. *et al.* Anodal transcranial direct current stimulation of prefrontal cortex enhances working memory. *Experimental Brain Research*. **166** (1), 23–30, doi: 10.1007/s00221-005-2334-6 (2005).
13. Fregni, F., Boggio, P.S., Nitsche, M.A., Marcolin, M.A., Rigonatti, S.P., Pascual-Leone, A. Treatment of major depression with transcranial direct current stimulation. *Bipolar Disorders*. **8** (2), 203–204, doi: 10.1111/j.1399-5618.2006.00291.x (2006).
14. Fritsch, B. *et al.* Direct Current Stimulation Promotes BDNF-Dependent Synaptic Plasticity: Potential Implications for Motor Learning. *Neuron*. **66** (2), 198–204, doi: 10.1016/j.neuron.2010.03.035 (2010).
15. Giordano, J. *et al.* Mechanisms and Effects of Transcranial Direct Current Stimulation. *Dose-Response*. **15** (1), 155932581668546, doi: 10.1177/1559325816685467 (2017).
16. Kabakov, A.Y., Muller, P.A., Pascual-Leone, A., Jensen, F.E., Rotenberg, A. Contribution of axonal orientation to pathway-dependent modulation of excitatory transmission by direct current stimulation in isolated rat hippocampus. *Journal of Neurophysiology*. **107** (7), 1881–1889, doi: 10.1152/jn.00715.2011 (2012).
17. Kampa, B.M., Clements, J., Jonas, P., Stuart, G.J. Kinetics of Mg<sup>2+</sup> unblock of NMDA receptors: implications for spike-timing dependent synaptic plasticity. *The Journal of Physiology*. **556** (2), 337–345, doi: 10.1113/jphysiol.2003.058842 (2004).
18. Lefaucheur, J.-P. *et al.* Evidence-based guidelines on the therapeutic use of transcranial direct current stimulation (tDCS). *Clinical Neurophysiology*. **128** (1), 56–92, doi: 10.1016/j.clinph.2016.10.087 (2017).
19. Marquez-Ruiz, J. *et al.* Transcranial direct-current stimulation modulates synaptic mechanisms involved in associative learning in behaving rabbits. *Proceedings of the National Academy of Sciences*. **109** (17), 6710–6715, doi: 10.1073/pnas.1121147109 (2012).
20. Meinzer, M., Lindenberg, R., Darkow, R., Ulm, L., Copland, D., Flöel, A. Transcranial Direct Current Stimulation and Simultaneous Functional Magnetic Resonance Imaging. *Journal of Visualized Experiments*. (86), e51730–e51730, doi: 10.3791/51730 (2014).
21. Monai, H. *et al.* Calcium imaging reveals glial involvement in transcranial direct current stimulation-induced plasticity in mouse brain. *Nature Communications*. **7**, 11100, doi: 10.1038/ncomms11100 (2016).



22. Nieratschker, V., Kiefer, C., Giel, K., Krüger, R., Plewnia, C. The COMT Val/Met Polymorphism Modulates Effects of tDCS on Response Inhibition. *Brain Stimulation*. **8** (2), 283–288, doi: 10.1016/j.brs.2014.11.009 (2015).
23. Nitsche, M.A. *et al.* Transcranial direct current stimulation: State of the art 2008. *Brain Stimulation*. **1** (3), 206–223, doi: 10.1016/j.brs.2008.06.004 (2008).
24. Nitsche, M.A. *et al.* Facilitation of implicit motor learning by weak transcranial direct current stimulation of the primary motor cortex in the human. *Journal of Cognitive Neuroscience*. **15** (4), 619–626, doi: 10.1162/089892903321662994 (2003).
25. Pelletier, S.J., Cicchetti, F. Cellular and Molecular Mechanisms of Action of Transcranial Direct Current Stimulation: Evidence from In Vitro and In Vivo Models. *International Journal of Neuropsychopharmacology*. **18** (2), pyu047-pyu047, doi: 10.1093/ijnp/pyu047 (2015).
26. Pereira, J.B. *et al.* Modulation of verbal fluency networks by transcranial direct current stimulation (tDCS) in Parkinson's disease. *Brain Stimulation*. **6** (1), 16–24, doi: 10.1016/j.brs.2012.01.006 (2013).
27. Rahman, A. *et al.* Cellular effects of acute direct current stimulation: Somatic and synaptic terminal effects. *Journal of Physiology*. **591** (10), 2563–2578, doi: 10.1113/jphysiol.2012.247171 (2013).
28. Sarmiento, C.I., San-Juan, D., Prasath, V.B.S. Letter to the Editor: Brief history of transcranial direct current stimulation (tDCS): from electric fishes to microcontrollers. *Psychological Medicine*. **46** (15), 3259–3261, doi: 10.1017/S0033291716001926 (2016).
29. Stagg, C.J., Jayaram, G., Pastor, D., Kincses, Z.T., Matthews, P.M., Johansen-Berg, H. Polarity and timing-dependent effects of transcranial direct current stimulation in explicit motor learning. *Neuropsychologia*. **49** (5), 800–804, doi: 10.1016/j.neuropsychologia.2011.02.009 (2011).
30. Stagg, C.J., Nitsche, M.A. Physiological basis of transcranial direct current stimulation. *The Neuroscientist*. **17** (1), 37–53, doi: 10.1177/1073858410386614 (2011).
31. Tortella, G. Transcranial direct current stimulation in psychiatric disorders. *World journal of psychiatry*. **5** (1), 88–102, doi: 10.5498/wjp.v5.i1.88 (2015).